SYSTEMS TECHNOLOGY, INC

13766 S. HAWTHORNE BOULEVARD • HAWTHORNE, CALIFORNIA 90250-7083 • PHONE (310) 679-2281
email: sti@systemstech.com FAX (310) 644-3887

Working Paper 1439-5

Investigation of suitable flight test inputs for system identification of low frequency dynamics for the miniMUTT

Started: January 14, 2015
Latest Revision: January 16, 2015

Dongchan Lee
Principal Specialist
310.679.2281x130

Brian P. Danowsky
Principal Research Engineer
310.679.2281x128

Prepared for

NASA NRA Grant:
Performance Adaptive Aeroelastic Wing
Contract No. NNX14AL36A

This page intentionally left blank

1.0 INTRODUCTION

The purpose of this document is to investigate suitable excitations for flight test to identify rigid body dynamic characteristics. It is understood that the stiff wing miniMUTT will be flown soon for identification of rigid body dynamic characteristic. The flight test data will further be used to identify unknown system parameters offline. The model system considered in this study is the BFF model at 40 kts as this is the lowest flight condition available and displays the least amount of coupling between rigid body and flexible dynamics. It is noted that this model still displays coupling between the pitch dynamics and the 1st symmetric wing bending mode. The objective is to focus on low frequency dynamics as it is expected that the stiff wing miniMUTT should display similar low frequency dynamics.

Different input sequences for the elevator and aileron control inputs, are investigated. The sensors investigated are the roll and pitch rates at the aircraft center body IMU.

2.0 ANALYSIS DESCRIPTION

Figure 1 to Figure 7 present frequency responses of roll and pitch rates from elevator chirp input only holding aileron to zero (computed by STI FFT-based frequency response estimator FREDA) and compared with the frequency responses of the truth model (BFF linear model at 40 kts). The data used to compute frequency response is the outputs of the truth model simulated with the inputs. The frequency responses of the pitch and roll rates match perfect with the truth model as shown in the figures.

Figure 8 to Figure 14 present frequency responses of roll and pitch rates from aileron chirp input only. Again, the match in the frequency responses between the truth and the estimated is excellent.

Figure 15 to Figure 23 show the response of each output to each input where both inputs are excited simultaneously. Roll rate from aileron and pitch rate from elevator show reasonably well match but the frequency response of cross-coupling axes show significant mismatch with very low coherence.

Figure 24 to Figure 30 compares the frequency responses estimated and the truth using pseudo random input. The estimated responses generally well follow the truth model but they are not as good as the chirp input cases. The same is observed when the aileron random input is used to simulate the vehicle responses. Again, significant mismatch has been observed when both elevator and aileron random inputs are used simultaneously to simulate the vehicle responses as shown in Figure 31 to Figure 46.

Figure 47 through Figure 69 include the same analysis above but with a much lower 50 Hz sample rate. In addition, the chirp frequencies range from 0 to 25 Hz (Nyquist limit, 157 rad/s). It is observed in the chirp input signals that amplitude is not captured in the higher frequencies. Fortunately, this does not have a very adverse effect on the identification results.

Other input sequences studied (all using 50 Hz sample rate):
Figure 70 to Figure 78: Orthogonal multi-sine sweep inputs for 3 seconds.
Figure 79 to Figure 85: Elevator 3-2-1-1 input for 23 seconds with pulse width 1 second.
Figure 86 to Figure 92: Aileron 3-2-1-1 input for 23 seconds with pulse width 1 second.

3.0 CONCLUSIONS

The simulation study presented here indicates that the nature of the input signal to excite the system is critical for estimating unknown system parameters. Although only frequency responses were identified and specific system parameters were not estimated, the quality of the rapidly determined frequency response serves as a good indicator of the ability to estimate parameters that are more specific (stability derivatives, etc.). In this study, a chirp signal works better than the random inputs. The 3-2-1-1 signal also displayed good identification results, arguably as good as the chirp results. In addition, it was observed that exciting both axes at the same time degrades the quality of estimated frequency responses. The orthogonal multi-sine with simultaneous inputs were attempted to remedy this issue but did not produce results notably better

than simultaneous chirps or random inputs. It is noted that degraded quality is only observed for the off-diagonal responses, which are of much lower amplitude and are less critical for traditional rigid body dynamics but will be more critical for the highly coupled flexible vehicle. It is suggested that in the actual flight test, the pilot or flight control system excite one axis at a time. In addition, to estimate the lift and drag characteristics such as the drag-polar of the system, pushover-pull up flight test is advisable due to its importance in flight performance.

4.0 RECOMMENDED FLIGHT TEST PLAN

It is understood that flight tests with the stiff wing vehicle will involve take off, flying the aircraft at constant altitude in a straight line for ~40 seconds, and then landing. The aircraft can be recovered and this flight profile can be repeated with a different test input. Due to the short duration, it is recommended to fly a single test input profile at a time.

Based on the analysis in this working paper with the BFF models at low speed, the following is the recommended order of test inputs with the [Matlab data file to use].* The amplitude in the files has been set to unity so this must be scaled appropriately. The ideal amplitude is as low as possible but large enough to obtain an adequately high signal to noise ratio.

1. Elevator chirp with no aileron input [chirp.mat]
2. Aileron chirp with no elevator input [chirp.mat]
3. Elevator 3-2-1-1 with no aileron input (0.5 second width) [D3211_05S.mat]
4. Aileron 3-2-1-1 with no elevator input (0.5 second width) [D3211_05S.mat]
5. Elevator 3-2-1-1 with no aileron input (1 second width) [D3211_1S.mat]
6. Aileron 3-2-1-1 with no elevator input (1 second width) [D3211_1S.mat]
7. Orthogonal multi-sine with simultaneous elevator and aileron inputs [orthogonal_multi_sine.mat]

* See file: ProposedInputSignal.zip for Matlab data files

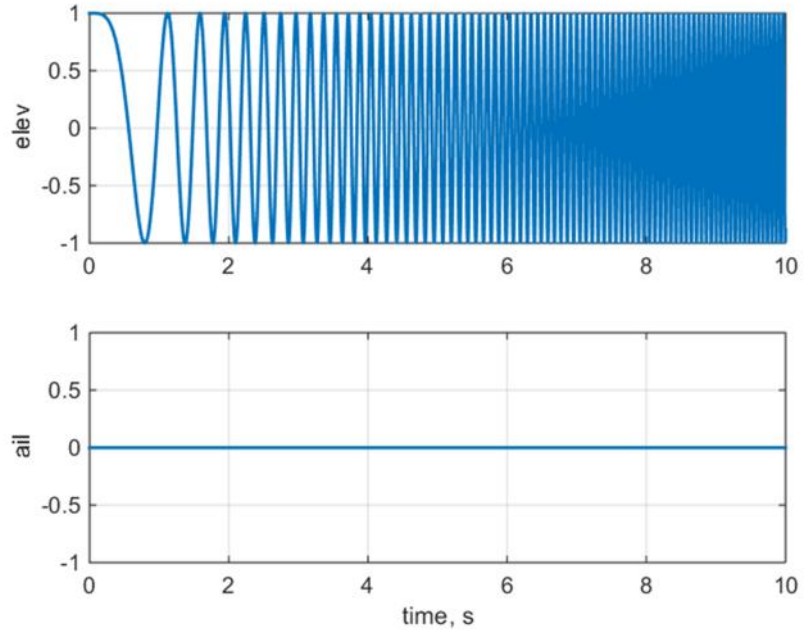

Figure 1: Control Input Time Histories.

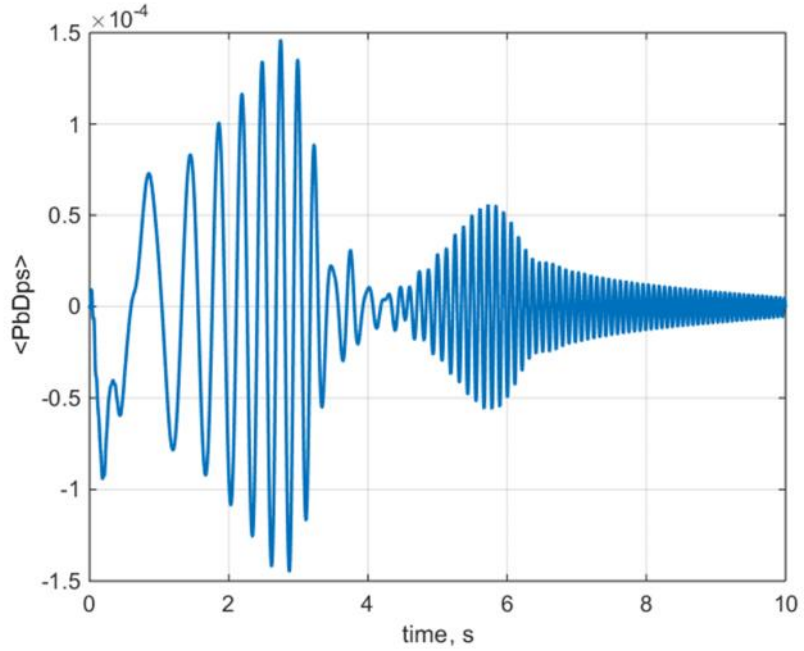

Figure 2: Roll Rate Response to Elevator Chirp Input.

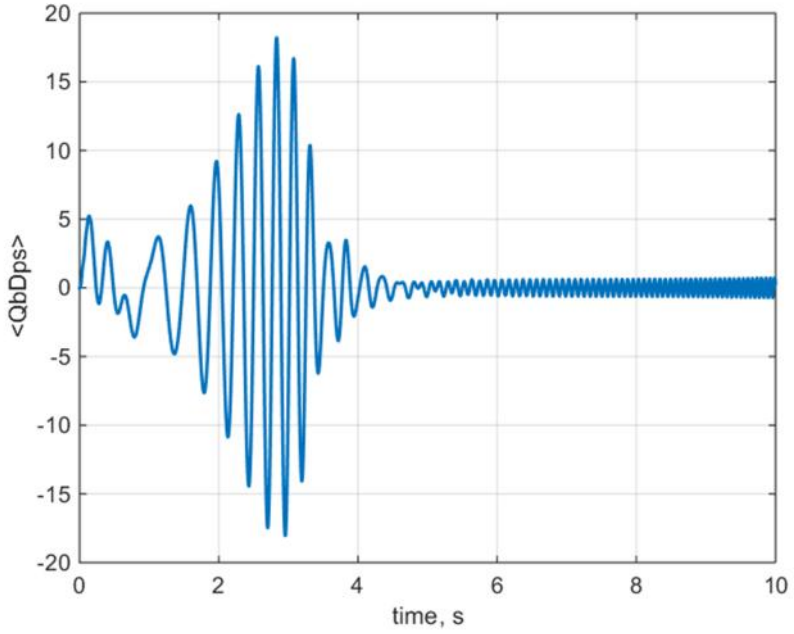

Figure 3: Pitch Rate Response to Elevator Chirp Input.

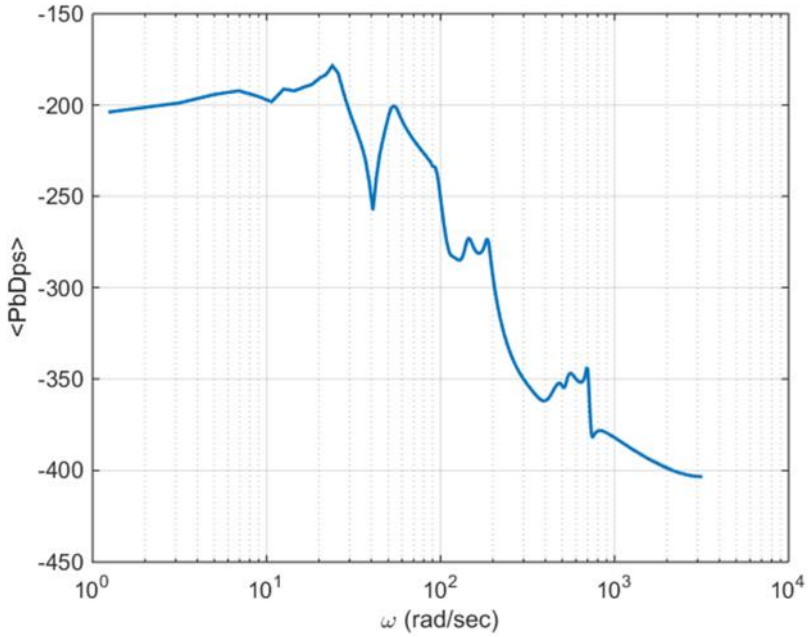

Figure 4: Power Spectral Density of Roll Rate to Elevator Chirp Input.

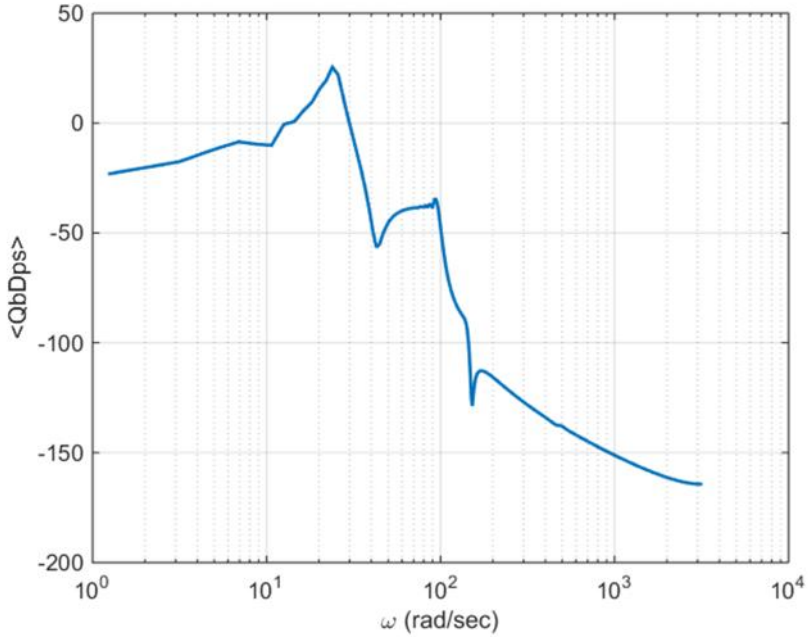

Figure 5: Power Spectral Density of Pitch Rate to Elevator Chirp Input.

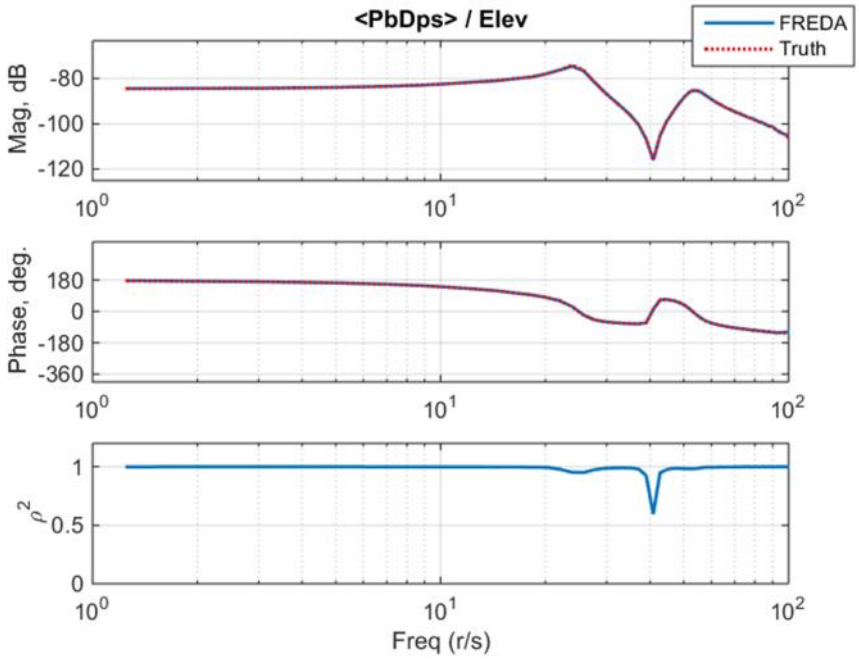

Figure 6: Frequency Response of Roll Rate to Elevator Chirp Input.

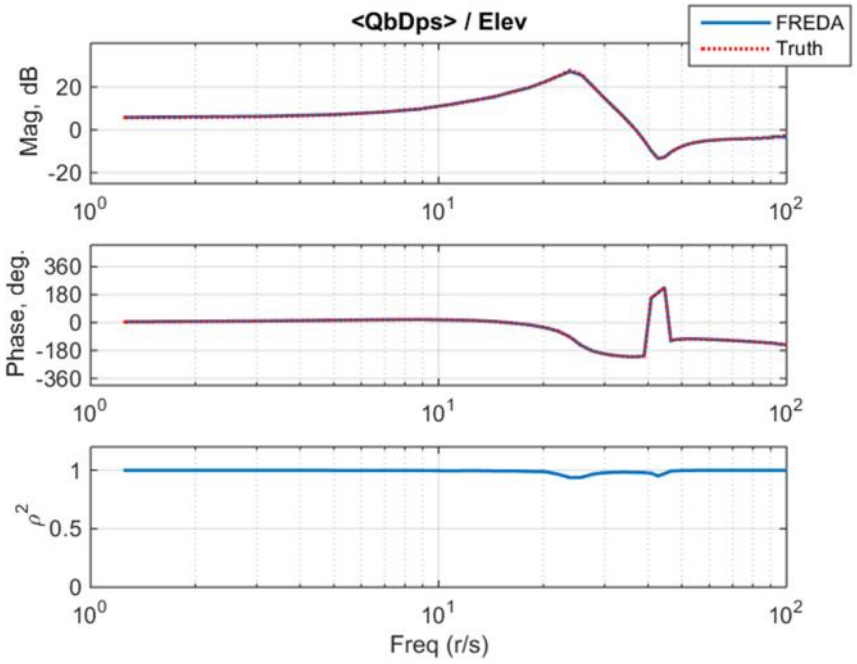

Figure 7: Frequency Response of Pitch Rate to Elevator Chirp Input.

(b) Aileron Chirp Signal only

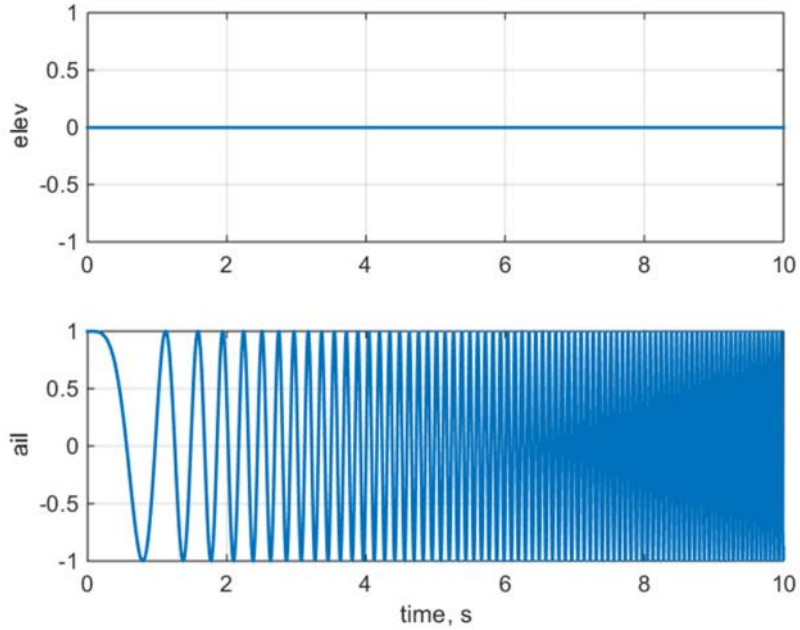

Figure 8: Control Input Time Histories.

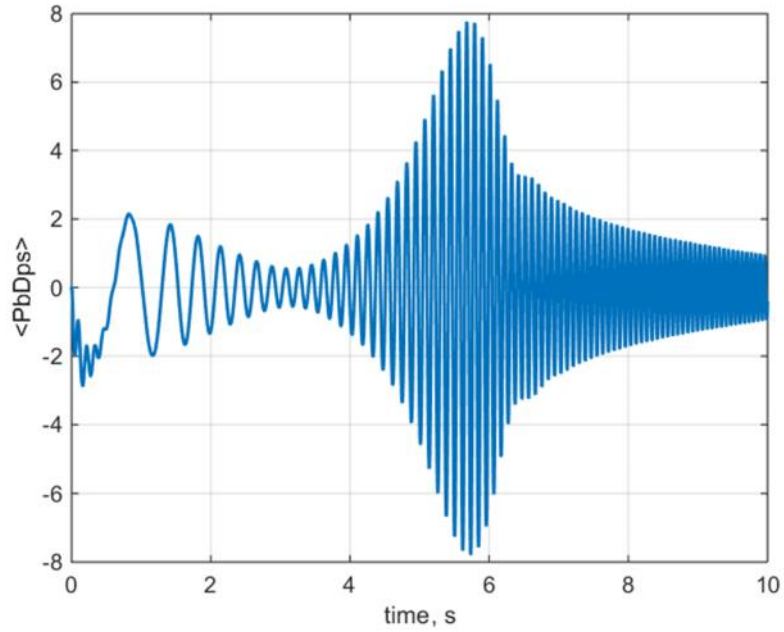

Figure 9: Roll Rate Response to Aileron Chirp Input.

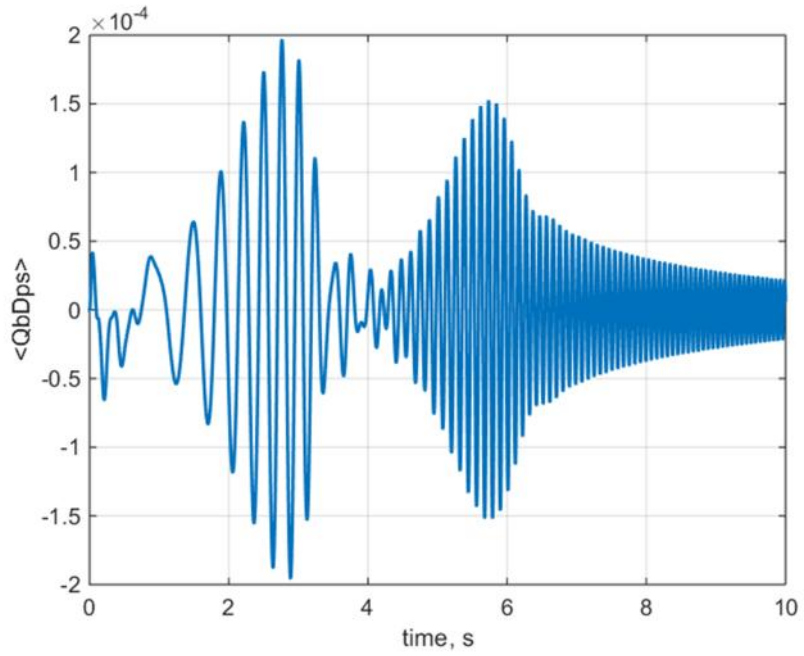

Figure 10: Pitch Rate Response to Aileron Chirp Input.

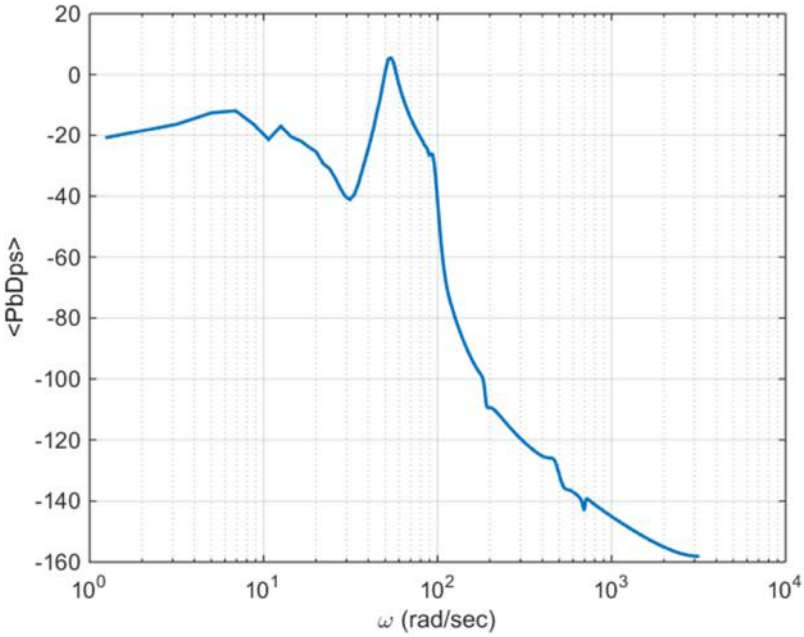

Figure 11: Power Spectral Density of Roll Rate to Aileron Chirp Input.

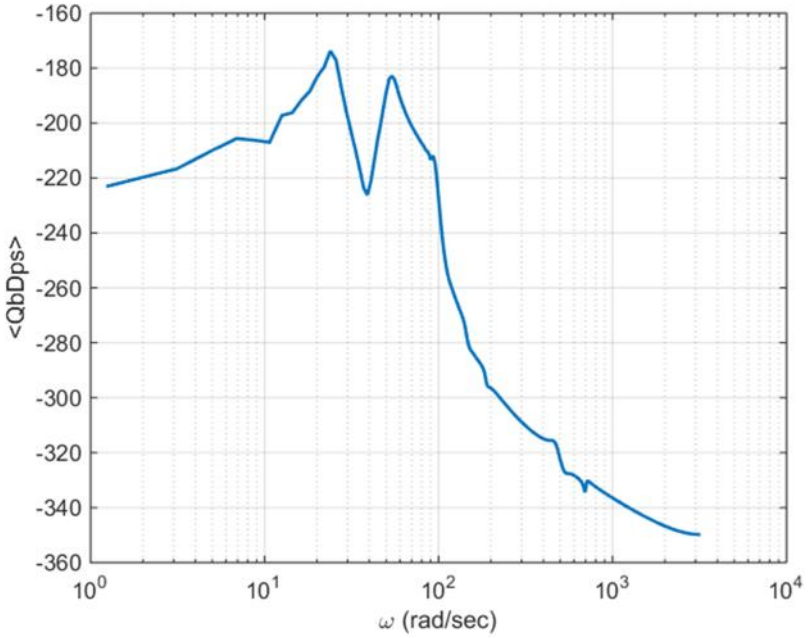

Figure 12: Power Spectral Density of Pitch Rate to Aileron Chirp Input.

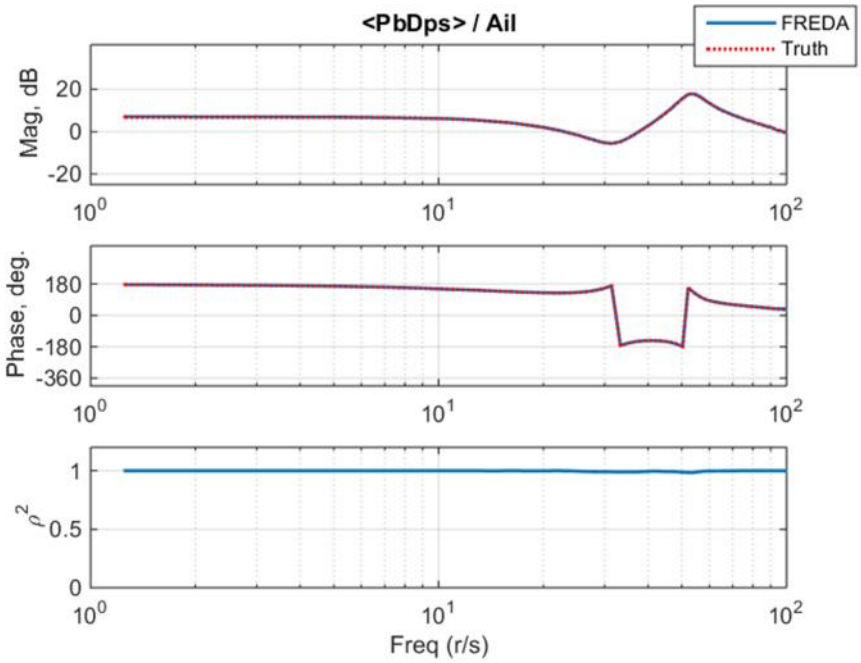

Figure 13: Frequency Response of Roll Rate to Aileron Chirp Input.

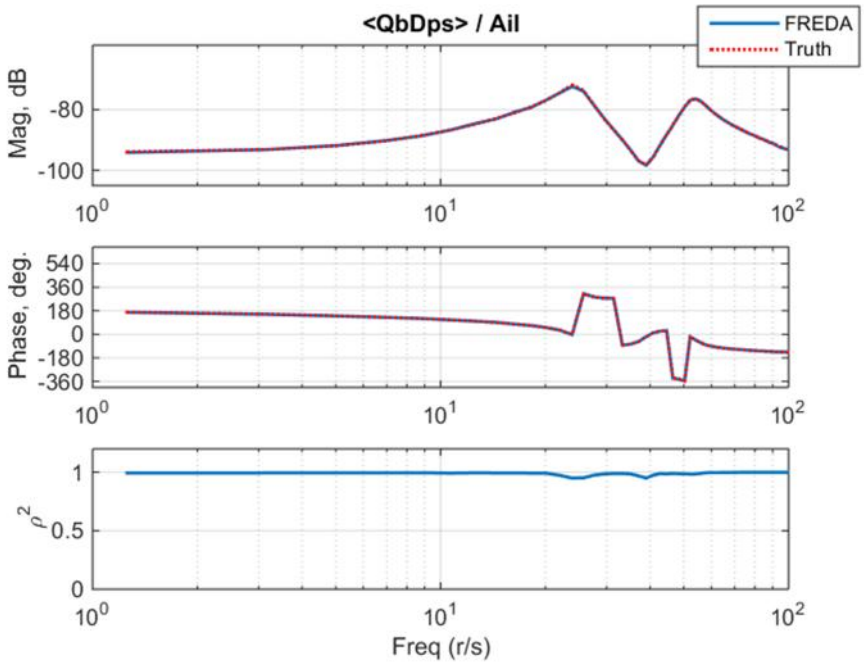

Figure 14: Frequency Response of Pitch Rate to Aileron Chirp Input.

(c) Elevator and Aileron Chirp Signal at the same time

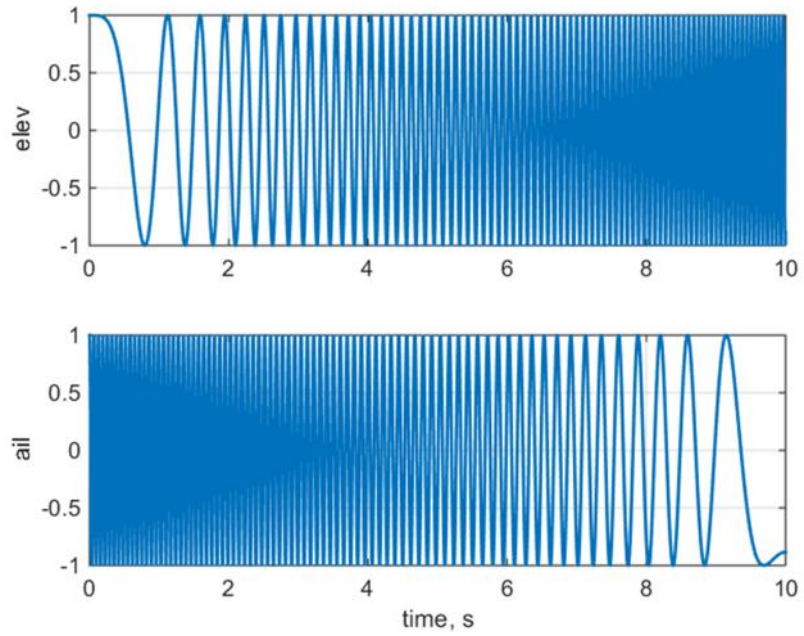

Figure 15: Control Input Time Histories.

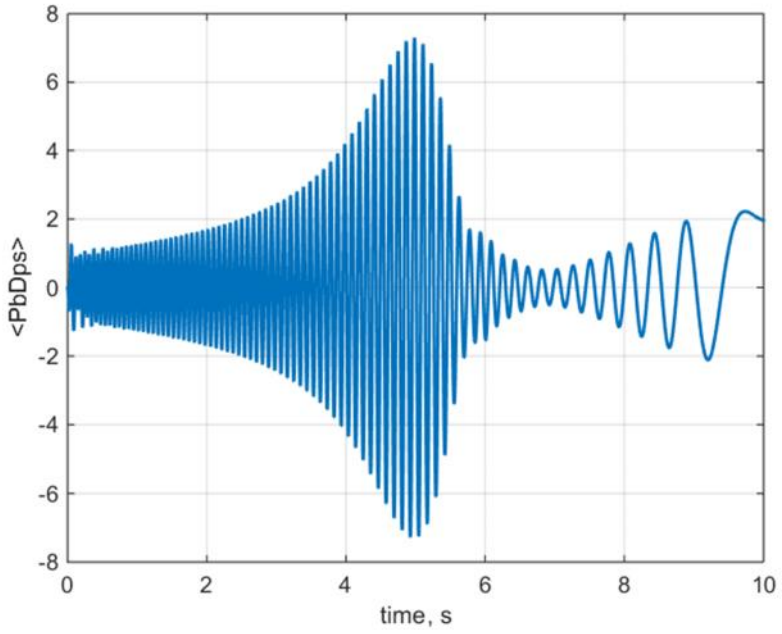

Figure 16: Roll Rate Response to Elevator and Aileron Chirp Inputs.

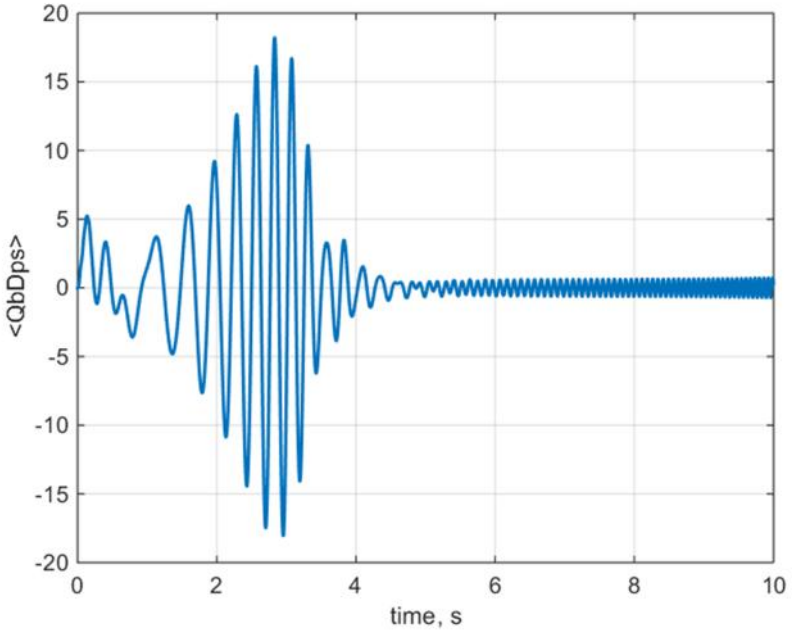

Figure 17: Pitch Rate Response to Elevator and Aileron Chirp Inputs.

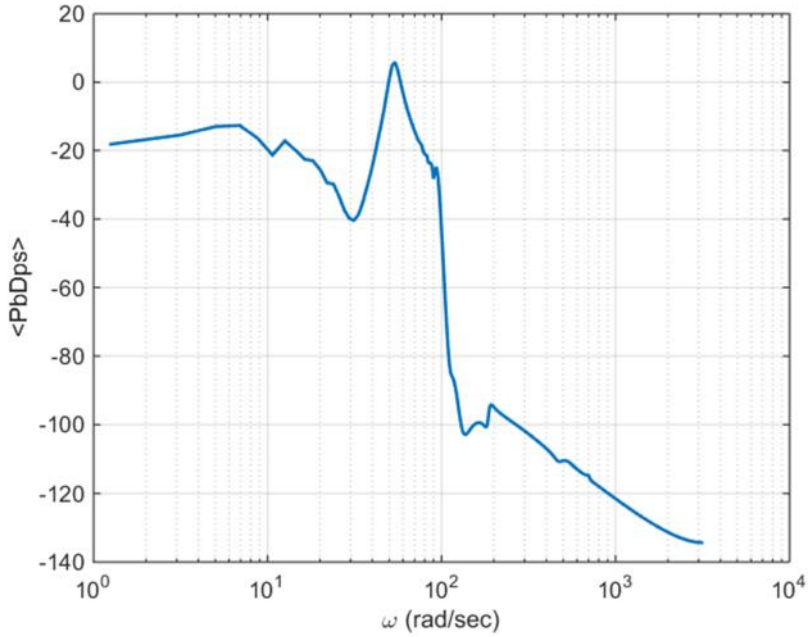

Figure 18: Power Spectral Density of Roll Rate to Elevator and Aileron Chirp Inputs.

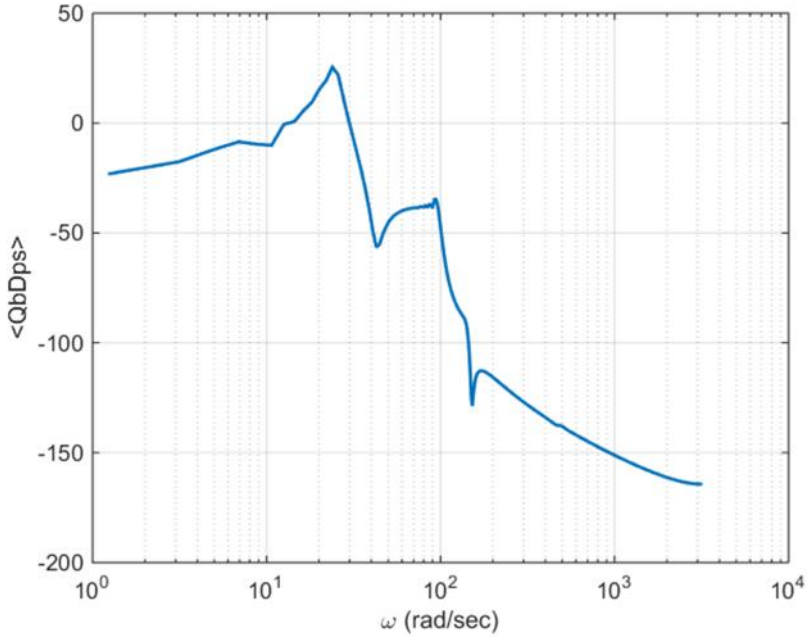

Figure 19: Power Spectral Density of Pitch Rate to Elevator and Aileron Chirp Inputs.

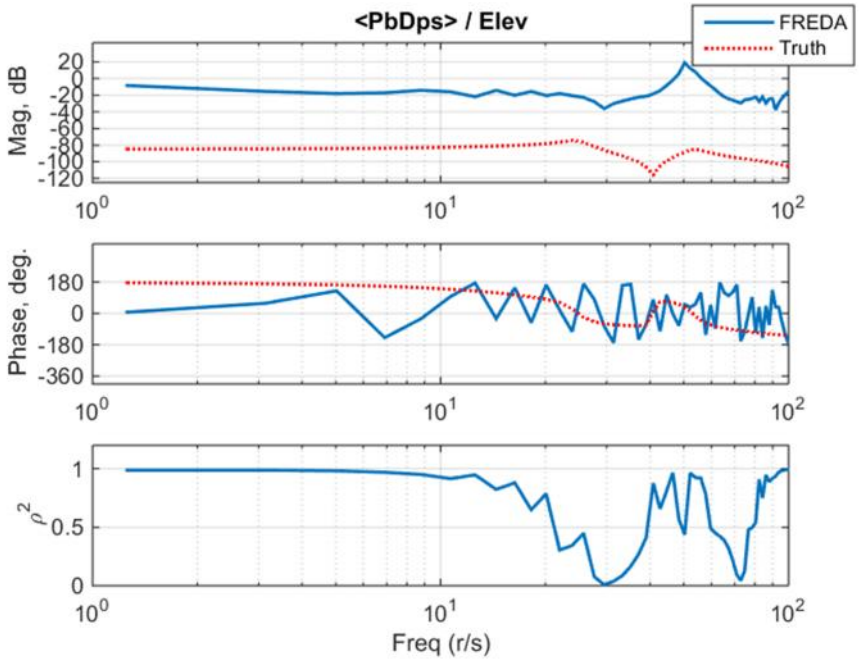

Figure 20: Frequency Response of Roll Rate to Elevator and Aileron Chirp Inputs.

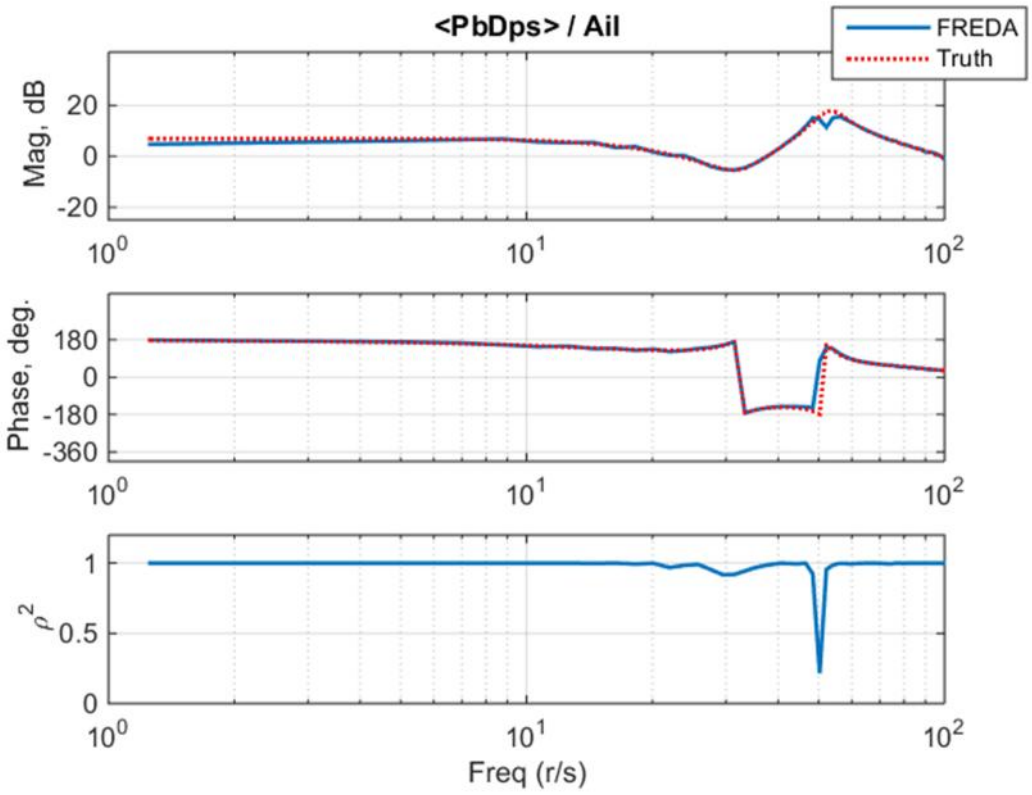

Figure 21: Frequency Response of Roll Rate to Elevator and Aileron Chirp Inputs.

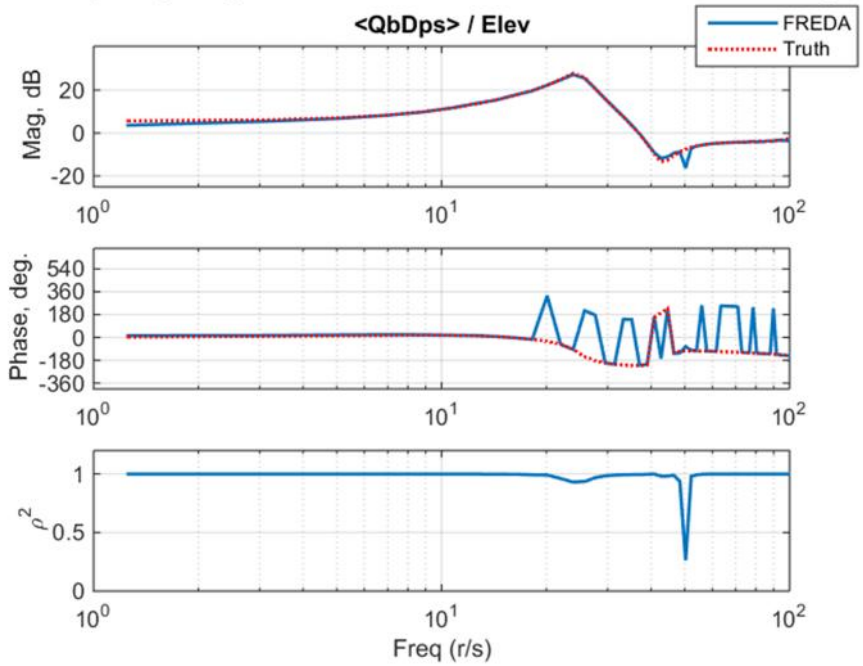

Figure 22: Frequency Response of Pitch Rate to Elevator and Aileron Chirp Inputs.

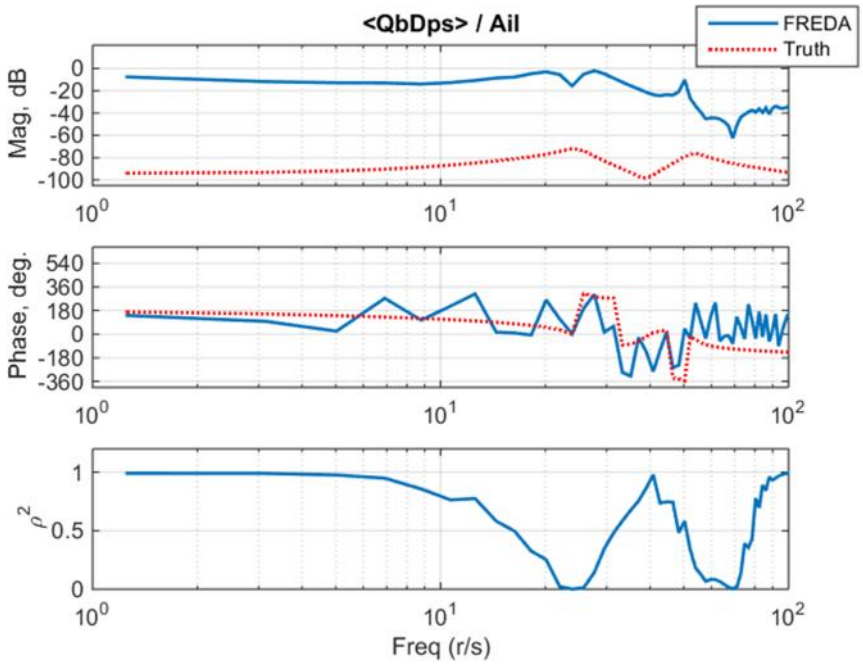

Figure 23: Frequency Response of Pitch Rate to Elevator and Aileron Chirp Inputs.

(1) Elevator and Aileron Random Input signal for 10 s
(a) Elevator Random Input Signal only

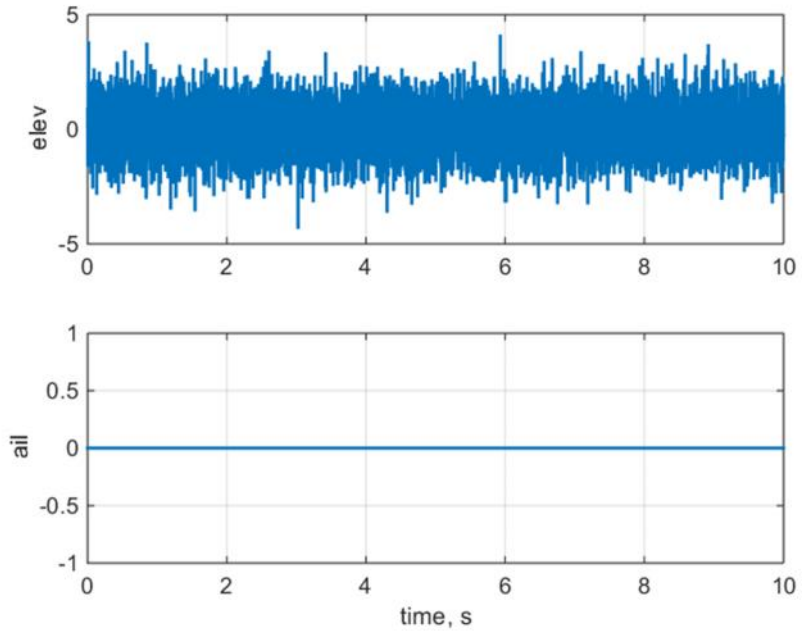

Figure 24: Control Input Time Histories.

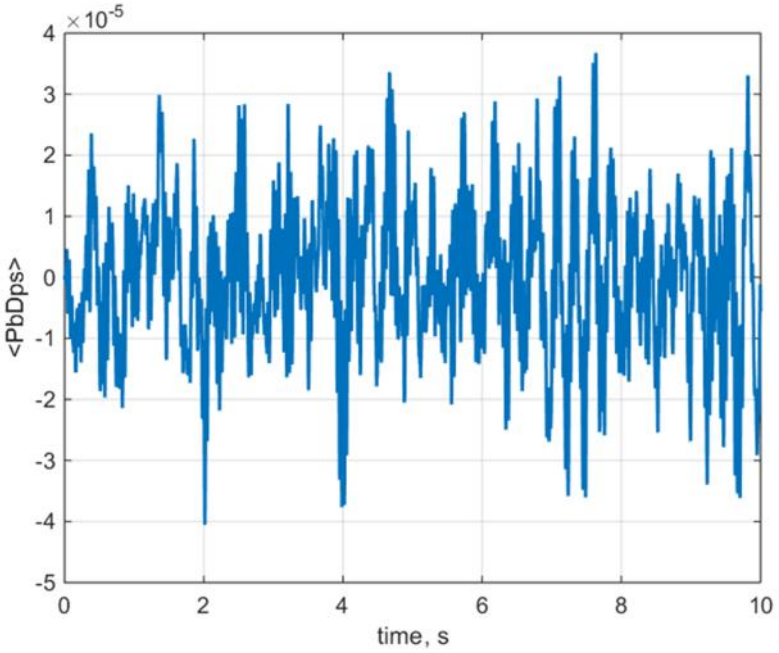

Figure 25: Roll Rate Response to Elevator Random Input.

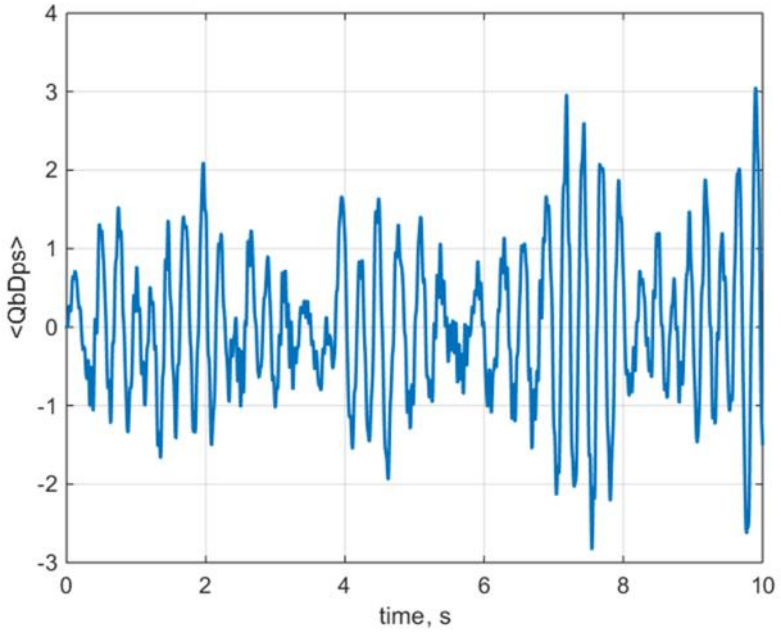

Figure 26: Pitch Rate Response to Elevator Random Input.

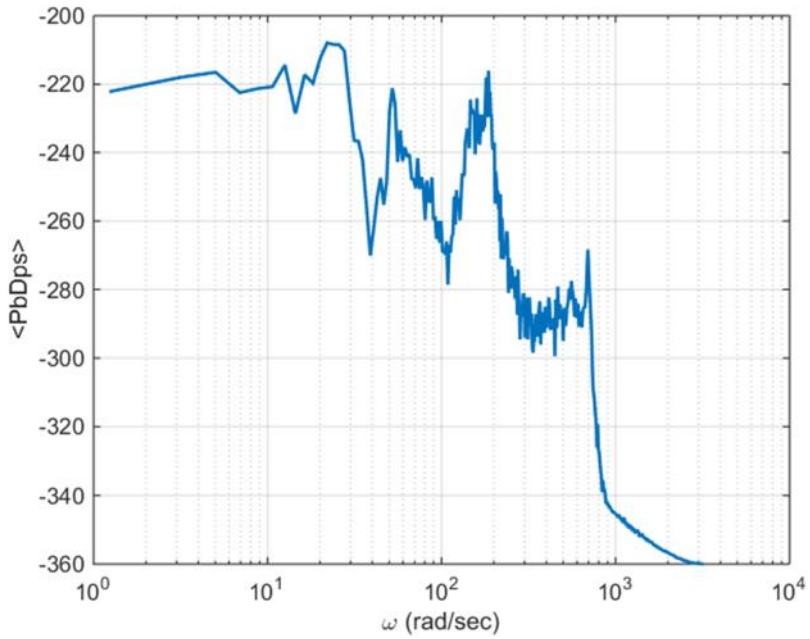

Figure 27: Power Spectral Density of Roll Rate to Elevator Random Input.

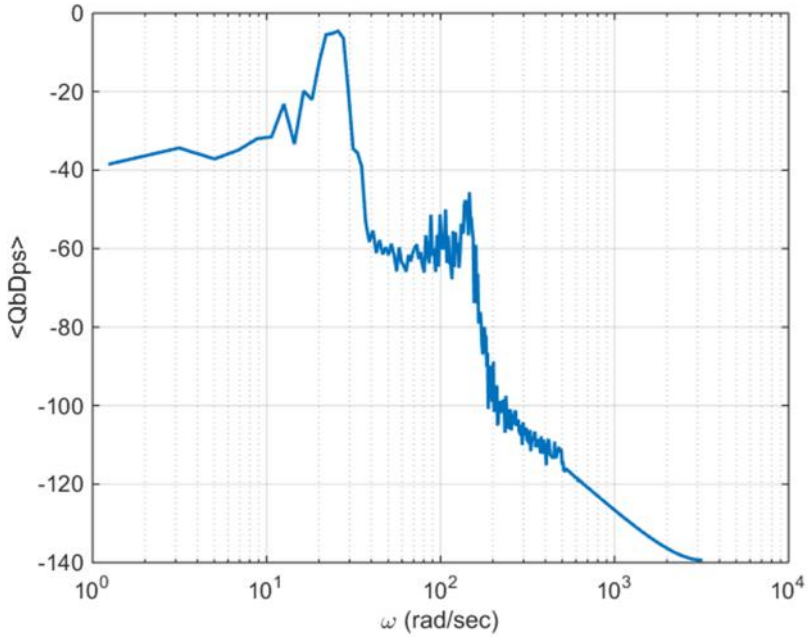

Figure 28: Power Spectral Density of Pitch Rate to Elevator Random Input.

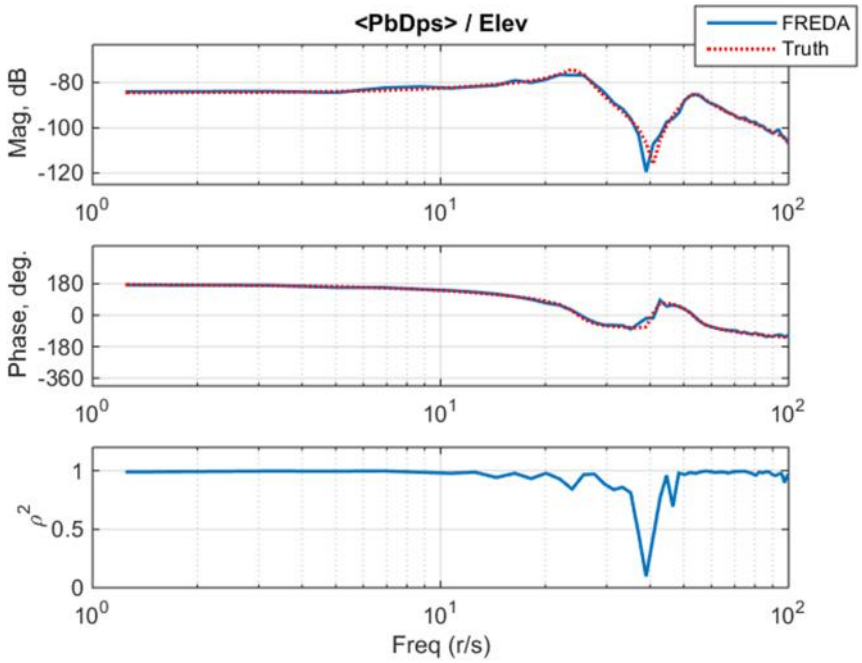

Figure 29: Frequency Response of Roll Rate to Elevator Random Input.

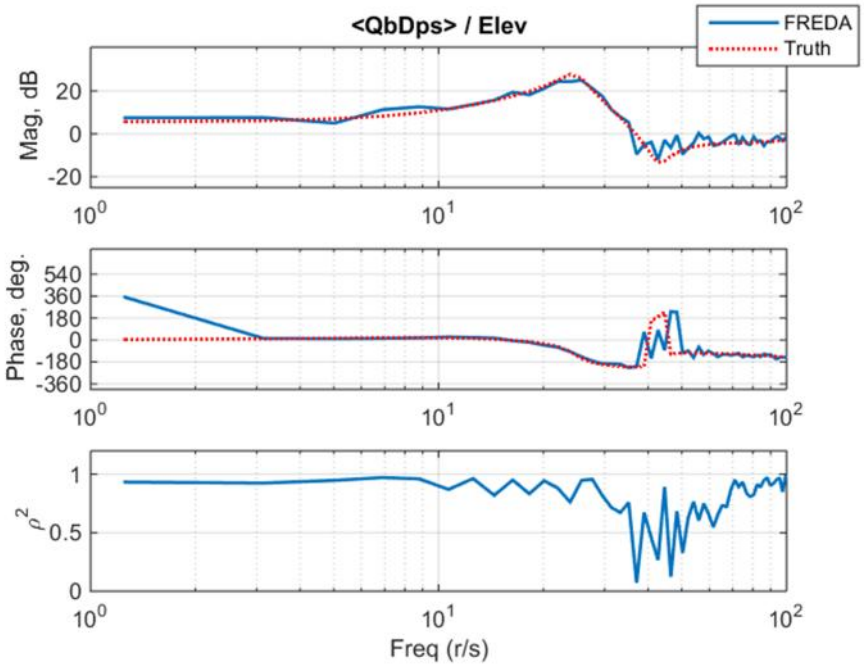

Figure 30: Frequency Response of Pitch Rate to Elevator Random Input.

(b) Aileron Random Input Signal only

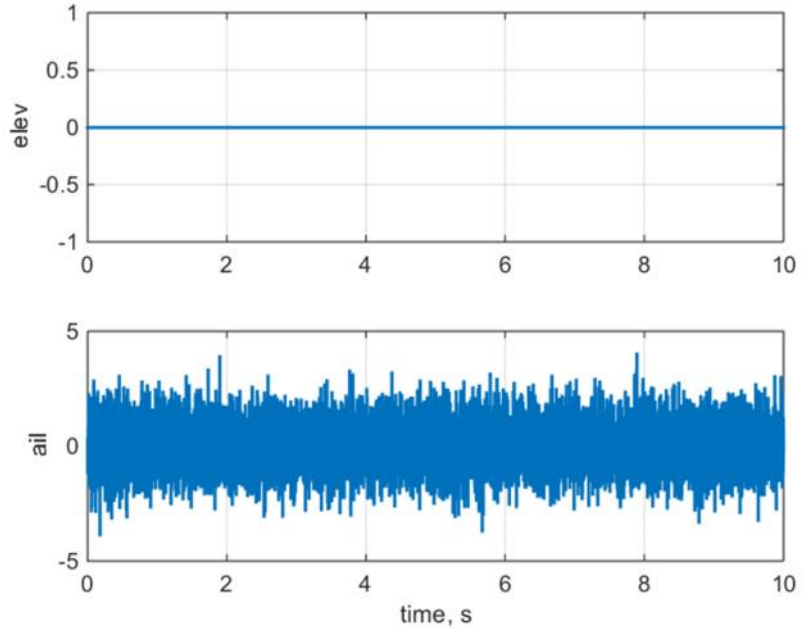

Figure 31: Control Input Time Histories.

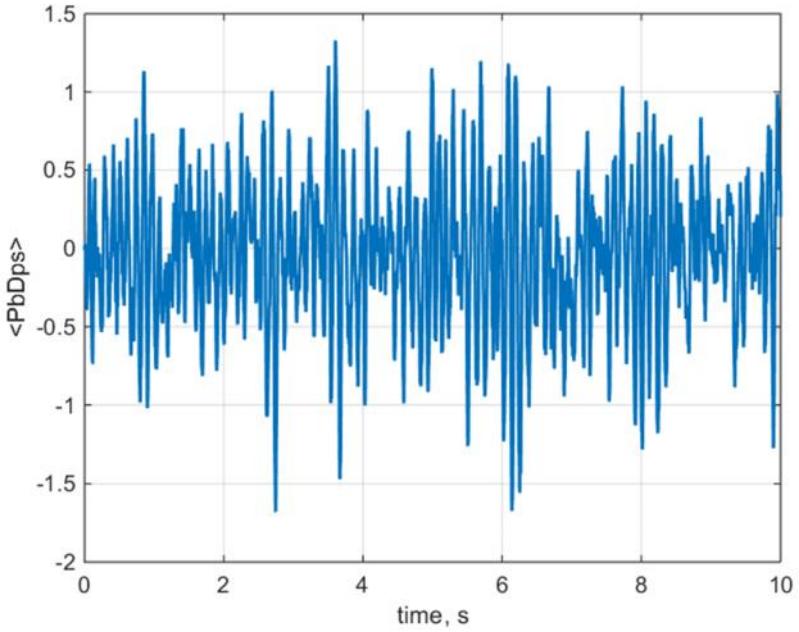

Figure 32: Roll Rate Response to Aileron Random Input.

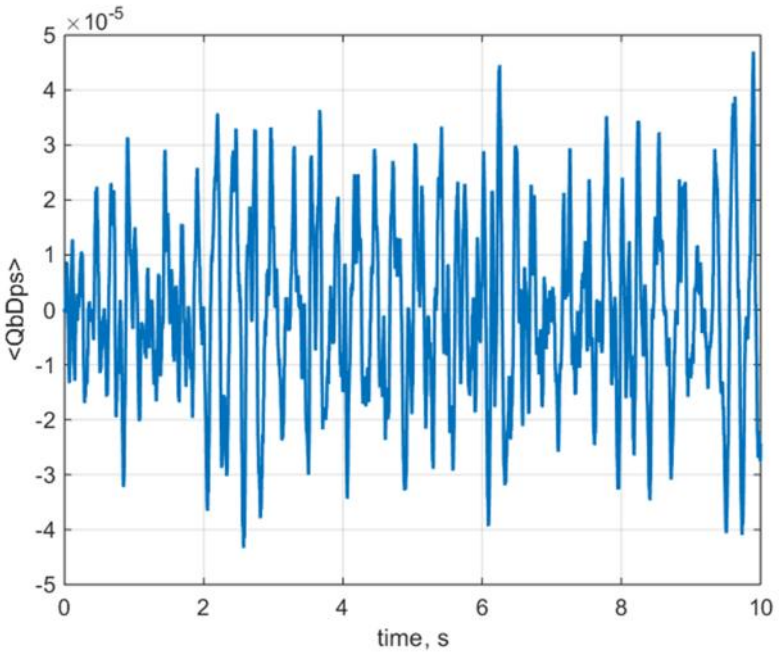

Figure 33: Pitch Rate Response to Aileron Random Input.

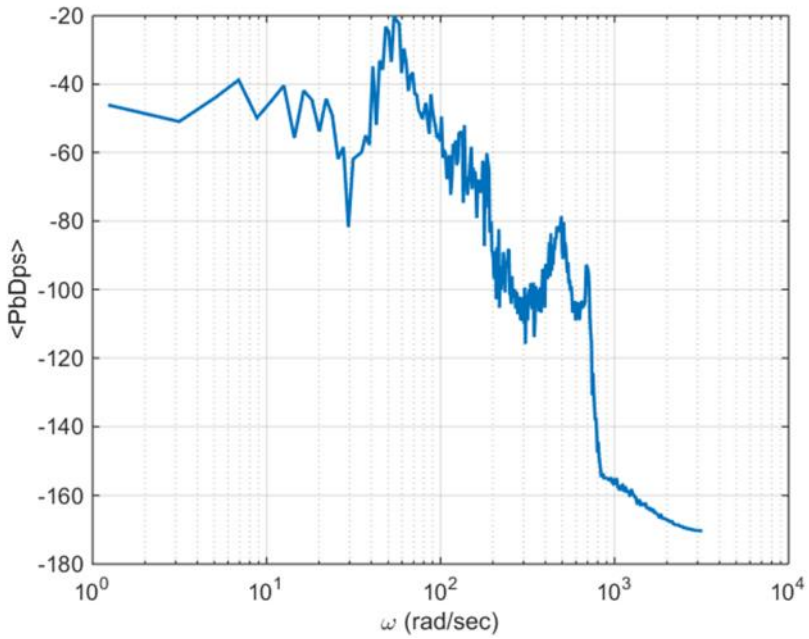

Figure 34: Power Spectral Density of Roll Rate to Aileron Random Input.

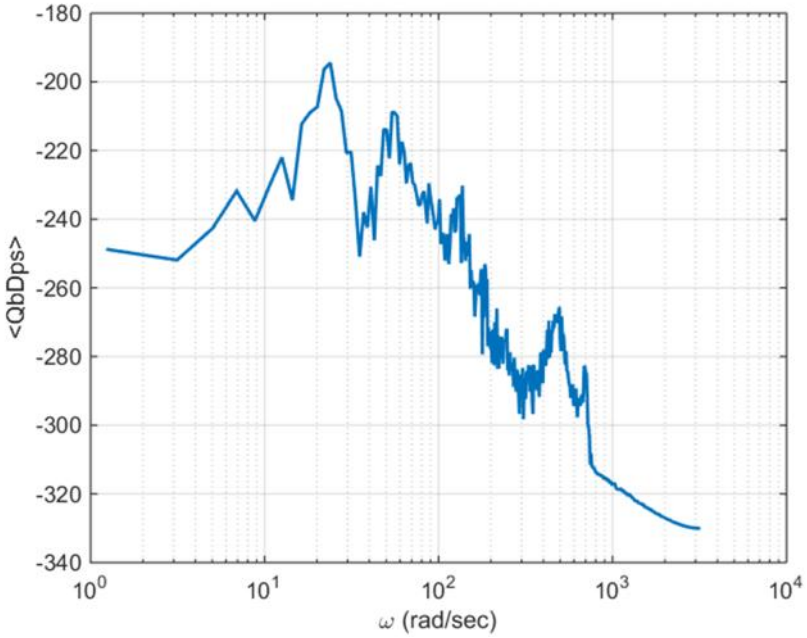

Figure 35: Power Spectral Density of Pitch Rate to Aileron Random Input.

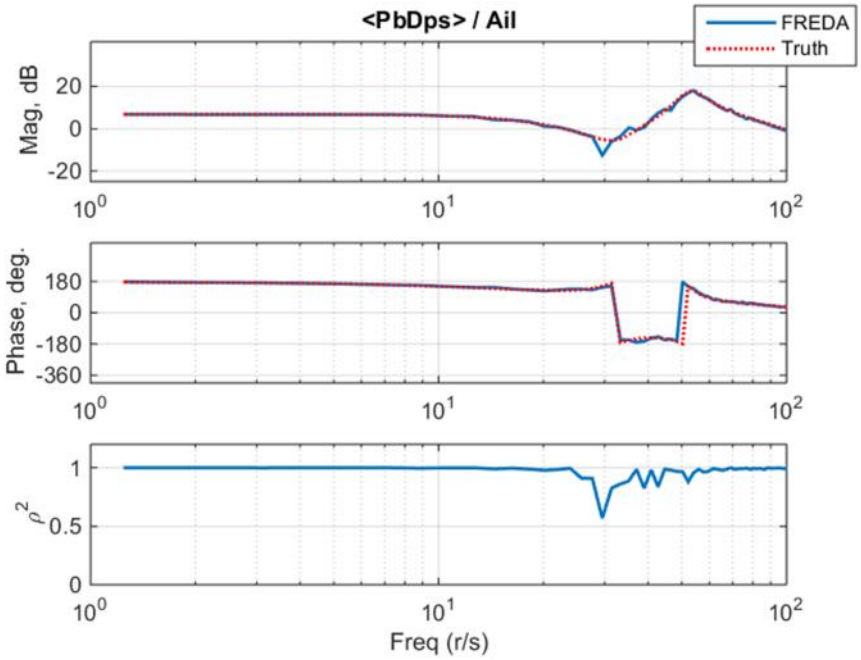

Figure 36: Frequency Response of Roll Rate to Aileron Random Input.

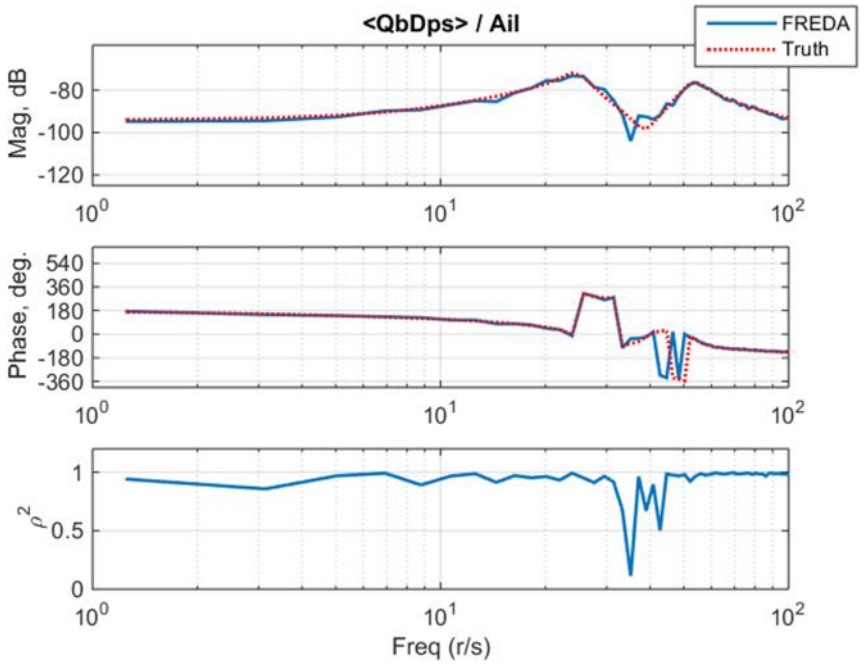

Figure 37: Frequency Response of Pitch Rate to Aileron Random Input.

(c) Elevator and Aileron Random Input Signal at the same time

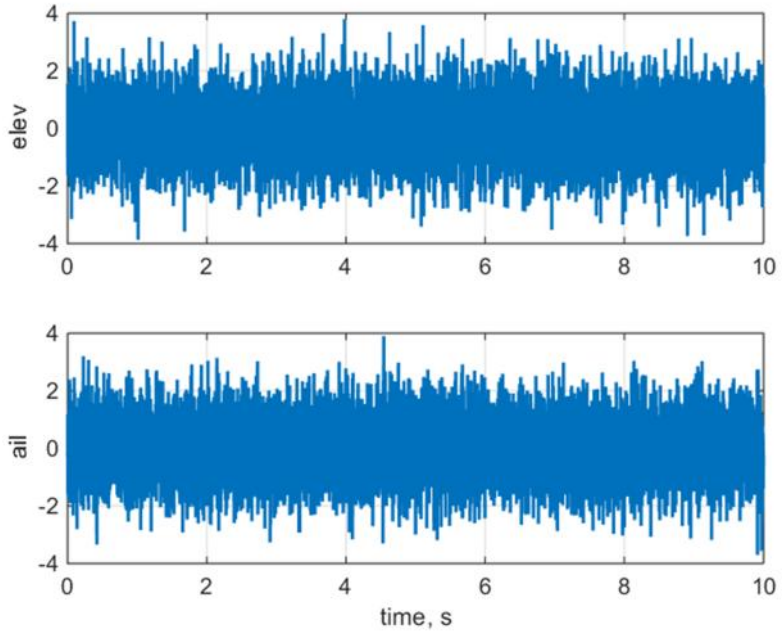

Figure 38: Control Input Time Histories.

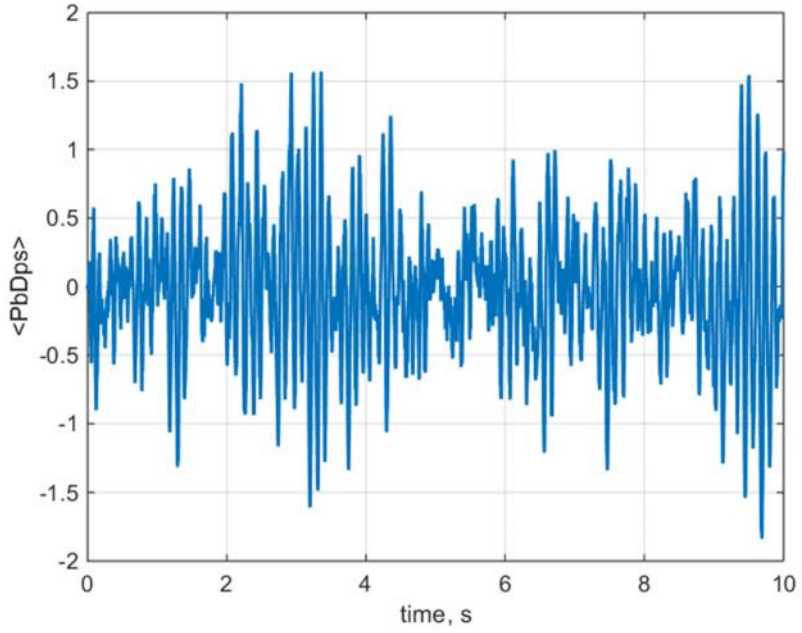

Figure 39: Roll Rate Response to Elevator and Aileron Random Inputs.

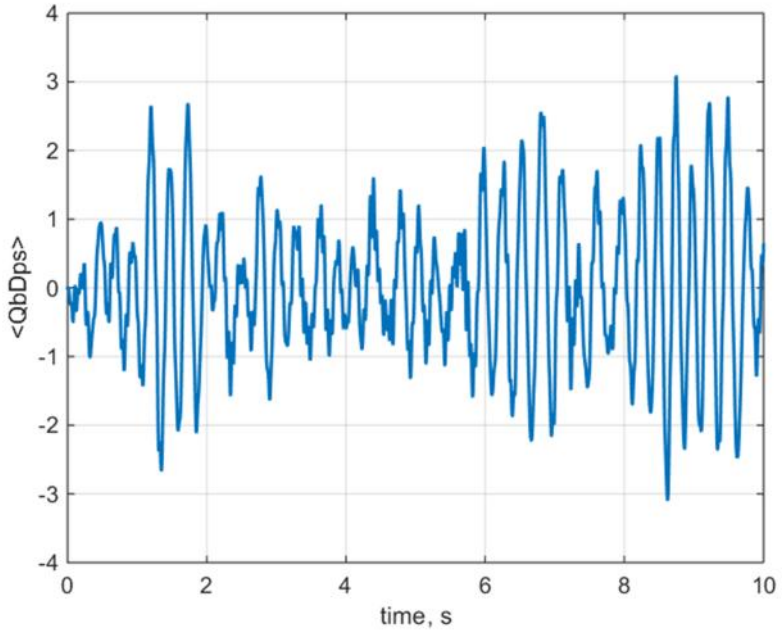

Figure 40: Pitch Rate Response to Elevator and Aileron Random Inputs.

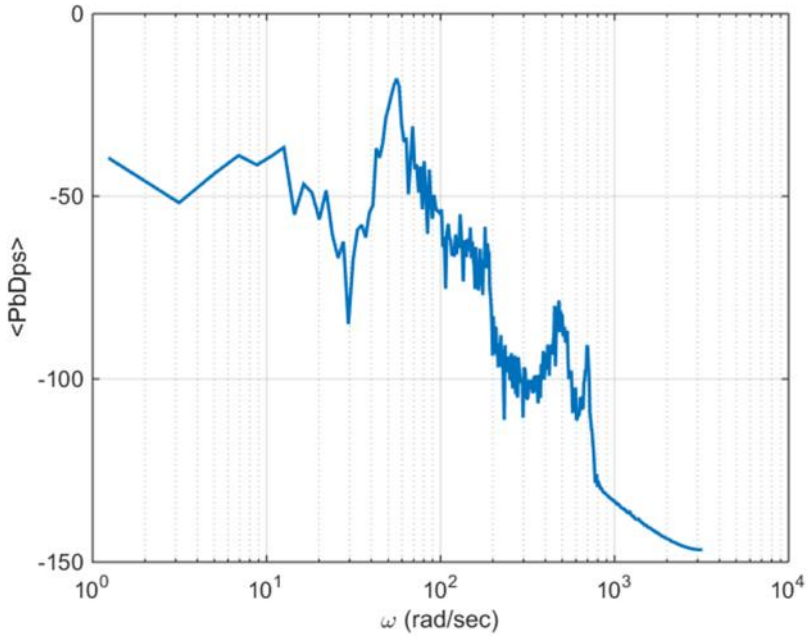

Figure 41: Power Spectral Density of Roll Rate to Elevator and Aileron Random Inputs.

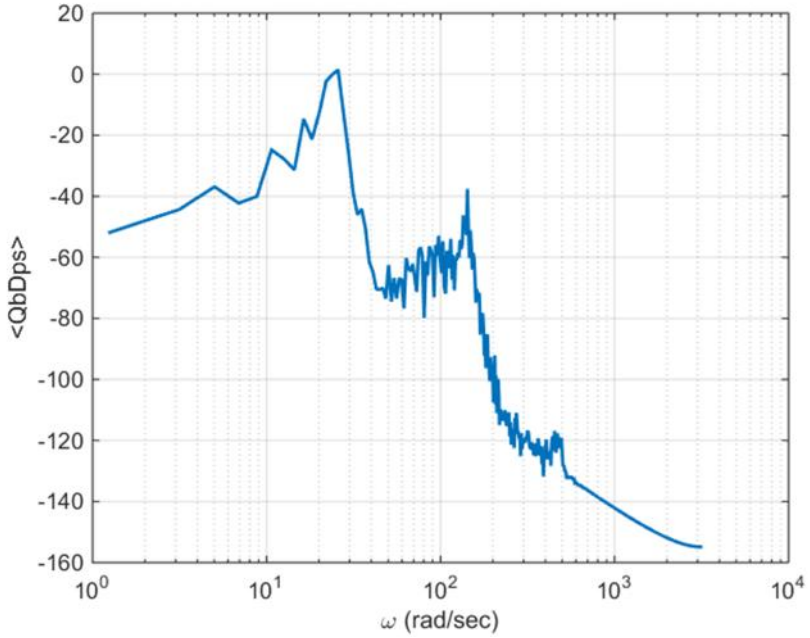

Figure 42: Power Spectral Density of Pitch Rate to Elevator and Aileron Random Inputs.

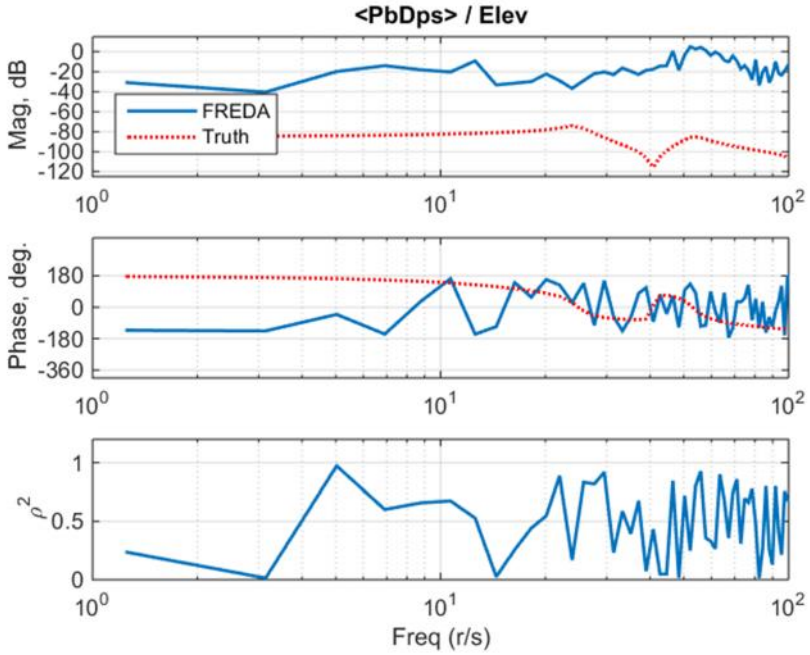

Figure 43: Frequency Response of Roll Rate to Elevator and Aileron Random Inputs.

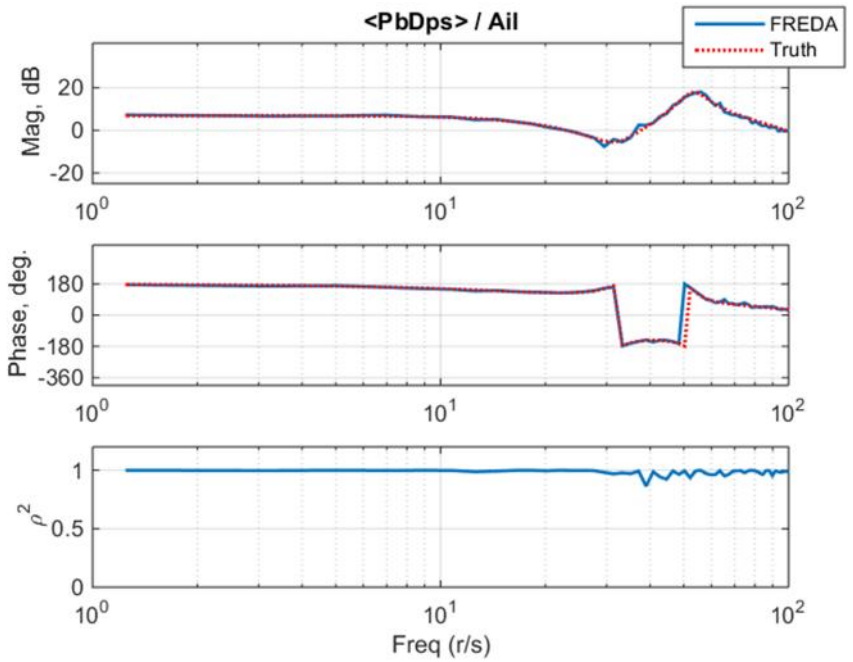

Figure 44: Frequency Response of Roll Rate to Elevator and Aileron Random Inputs.

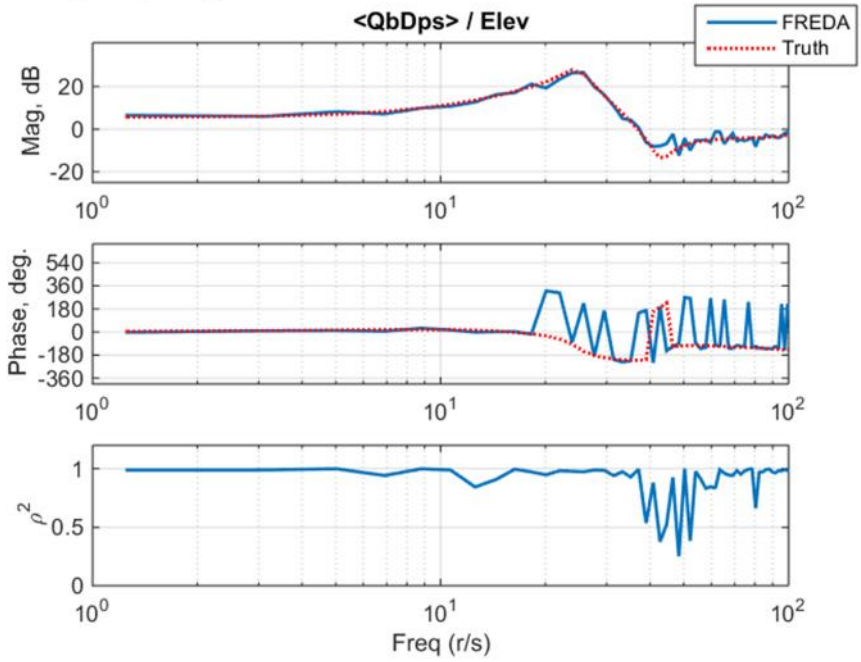

Figure 45: Frequency Response of Pitch Rate to Elevator and Aileron Random Inputs.

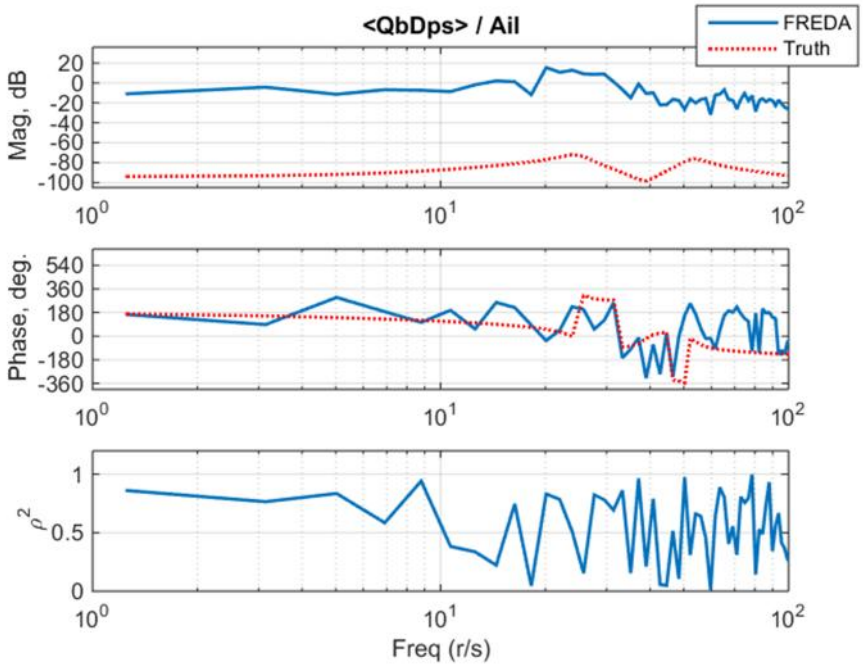

Figure 46: Frequency Response of Pitch Rate to Elevator and Aileron Random Inputs.

50 Hz

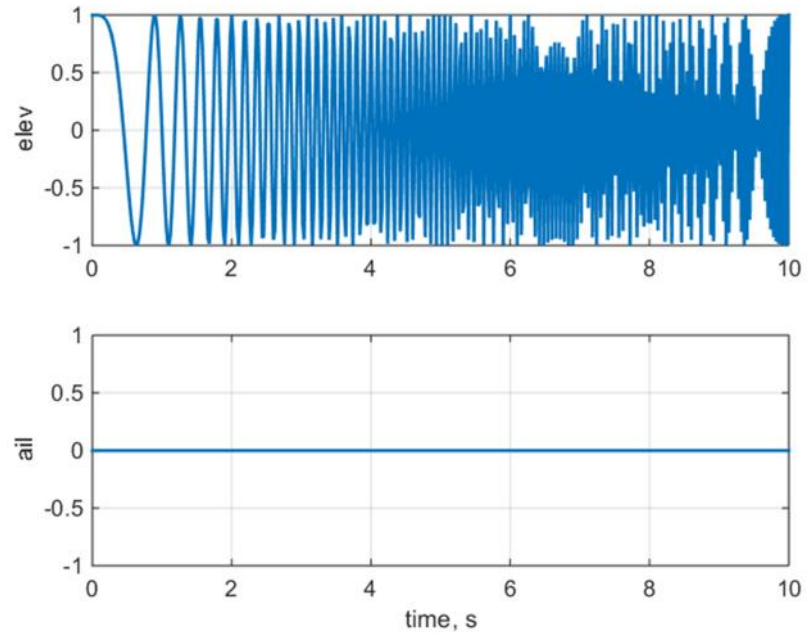

Figure 47: Control Input Time Histories.

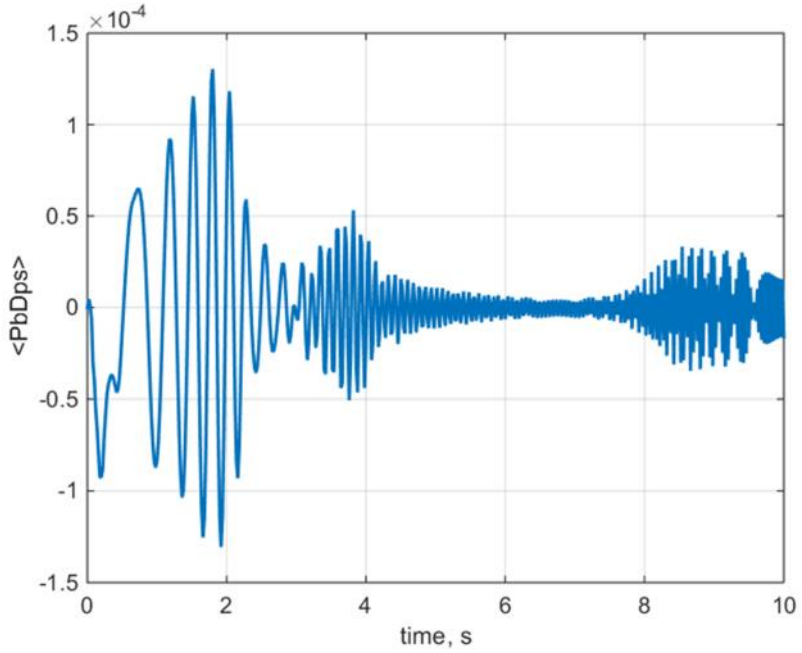

Figure 48: Roll Rate Response to Elevator Chirp Input.

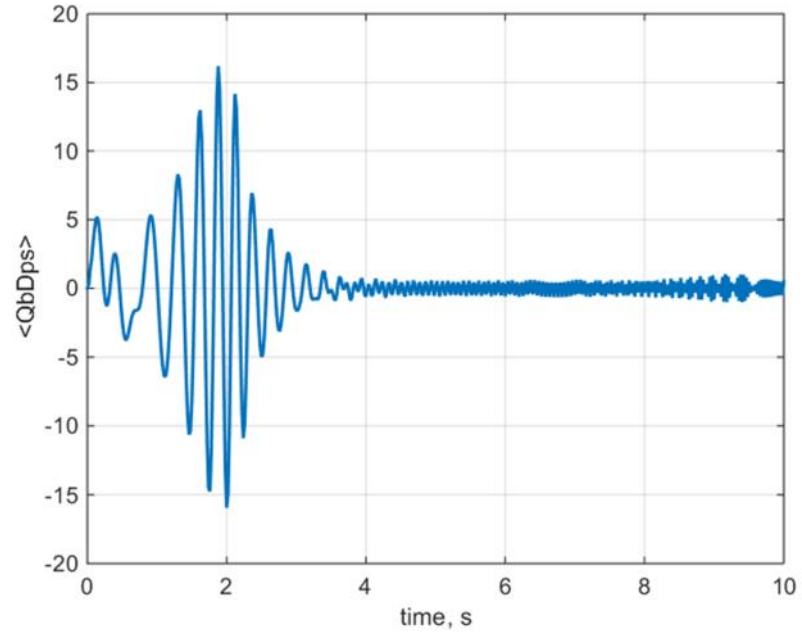

Figure 49: Pitch Rate Response to Elevator Chirp Input.

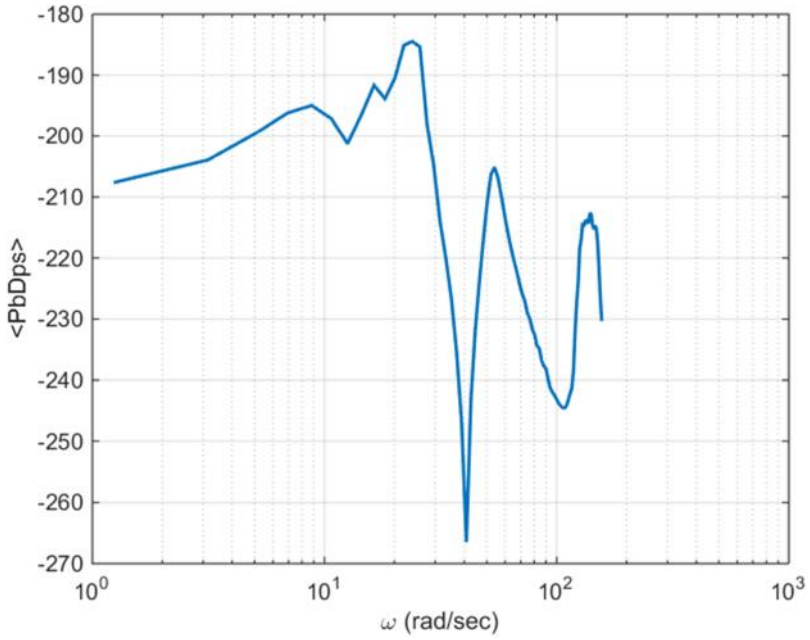

Figure 50: Power Spectral Density of Roll Rate to Elevator Chirp Input.

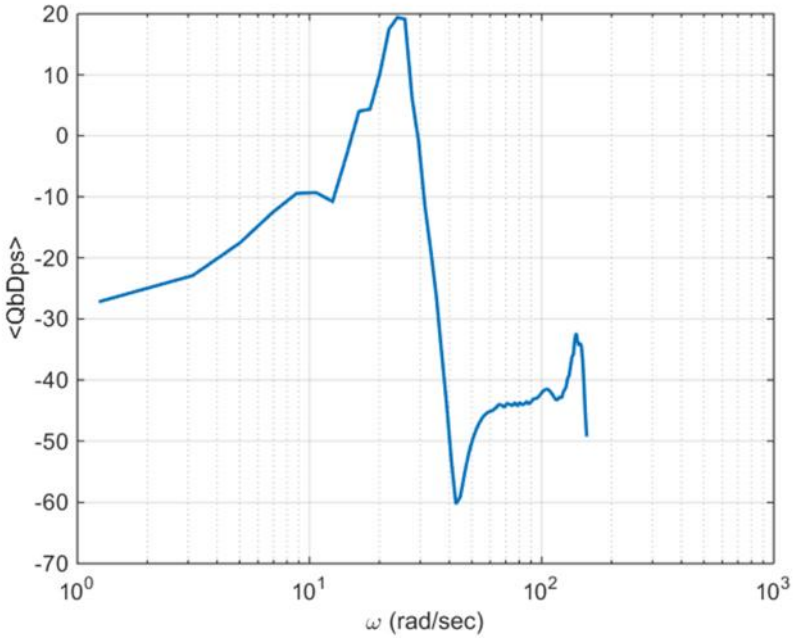

Figure 51: Power Spectral Density of Pitch Rate to Elevator Chirp Input.

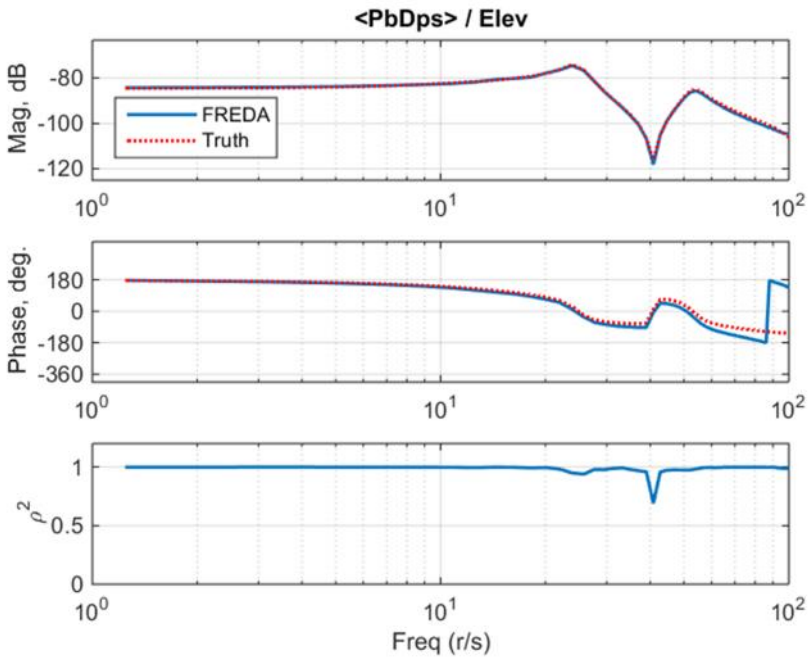

Figure 52: Frequency Response of Roll Rate to Elevator Chirp Input.

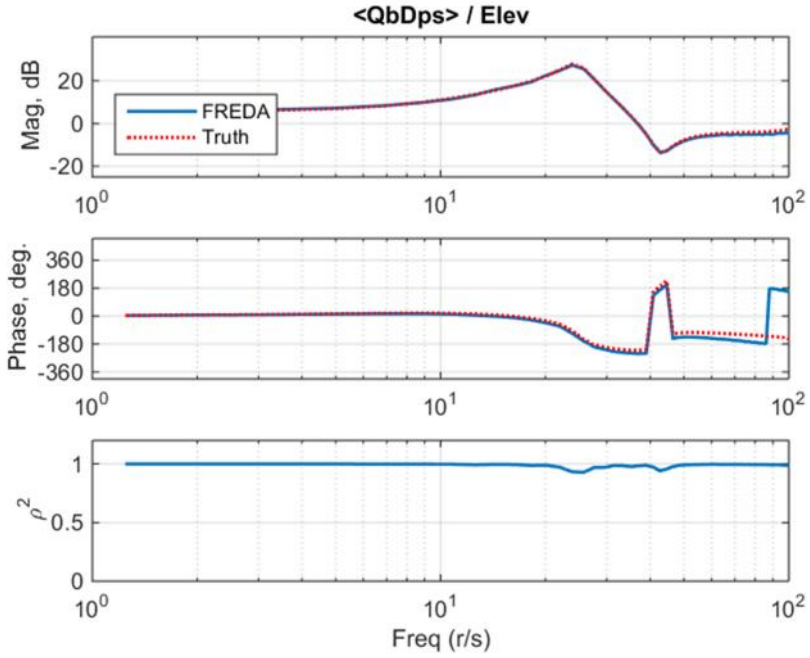

Figure 53: Frequency Response of Pitch Rate to Elevator Chirp Input.

(b) Aileron Chirp Signal only

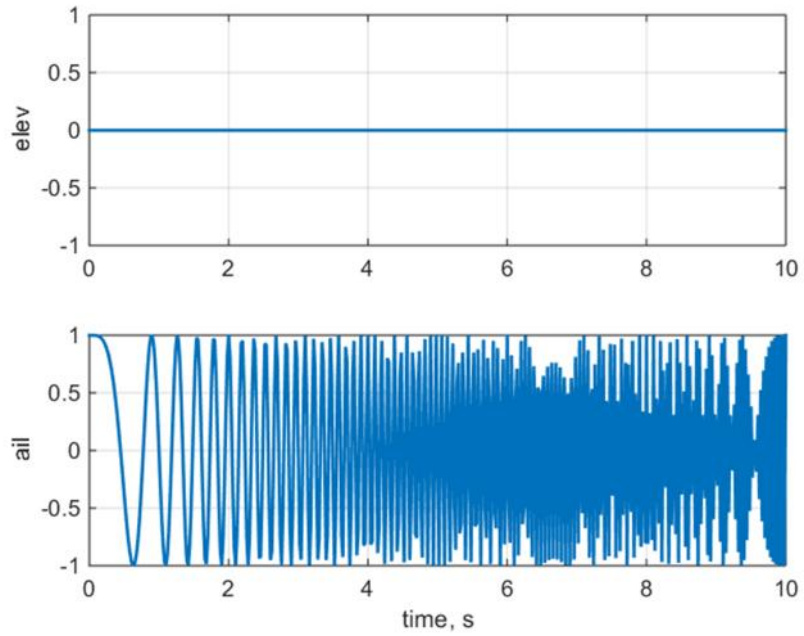

Figure 54: Control Input Time Histories.

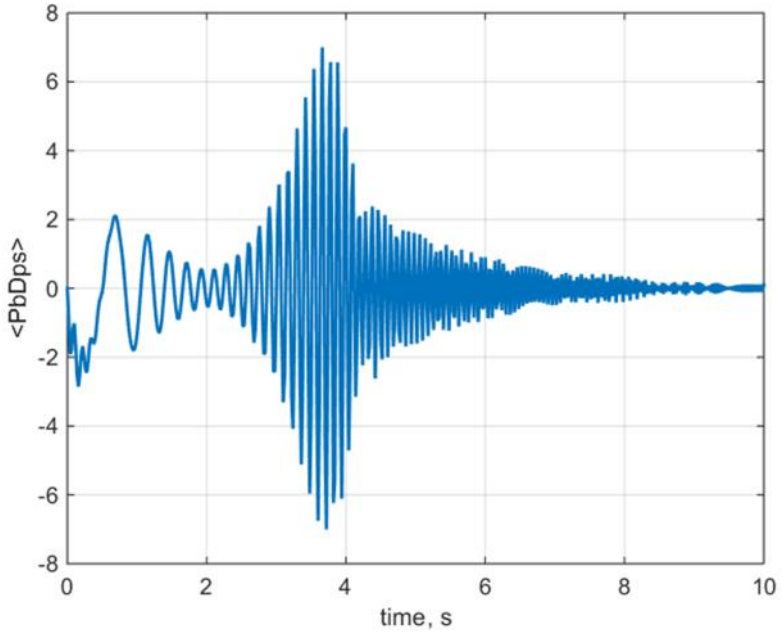

Figure 55: Roll Rate Response to Aileron Chirp Input.

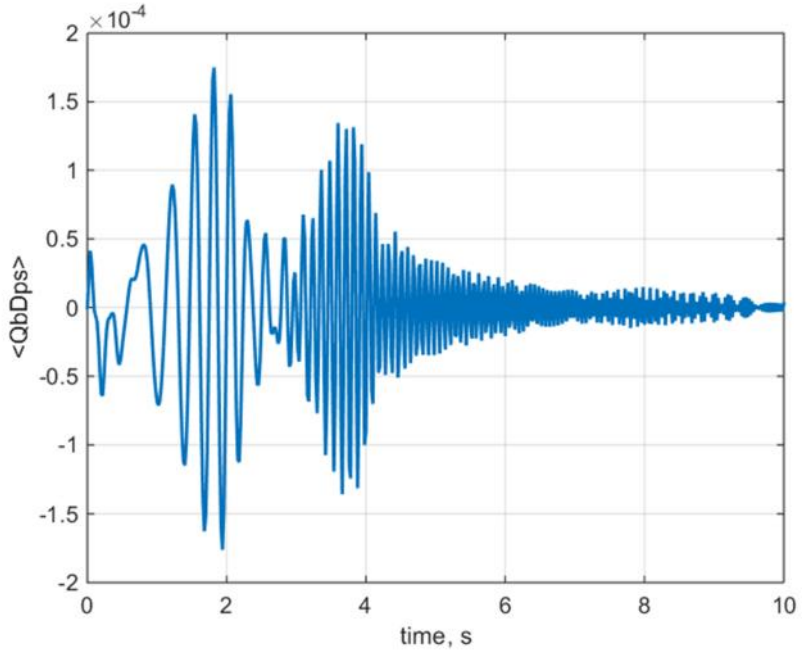

Figure 56: Pitch Rate Response to Aileron Chirp Input.

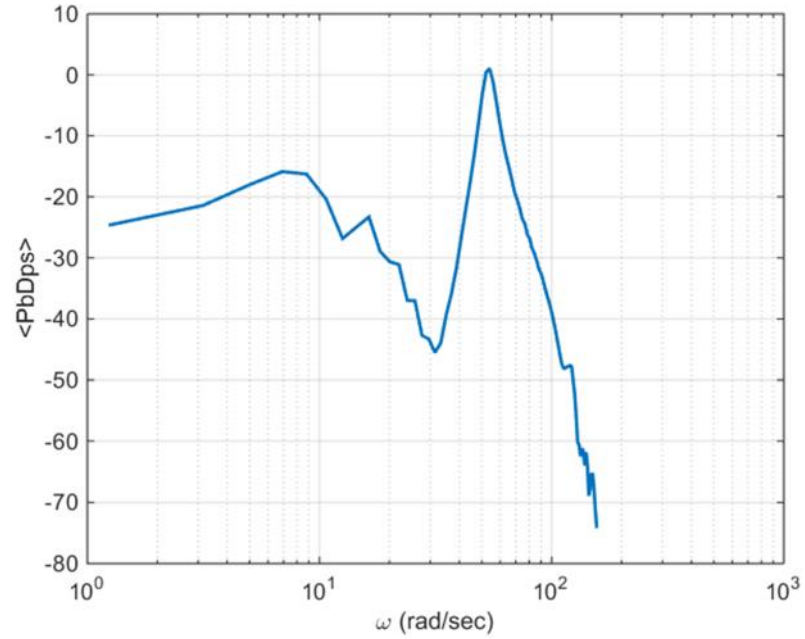

Figure 57: Power Spectral Density of Roll Rate to Aileron Chirp Input.

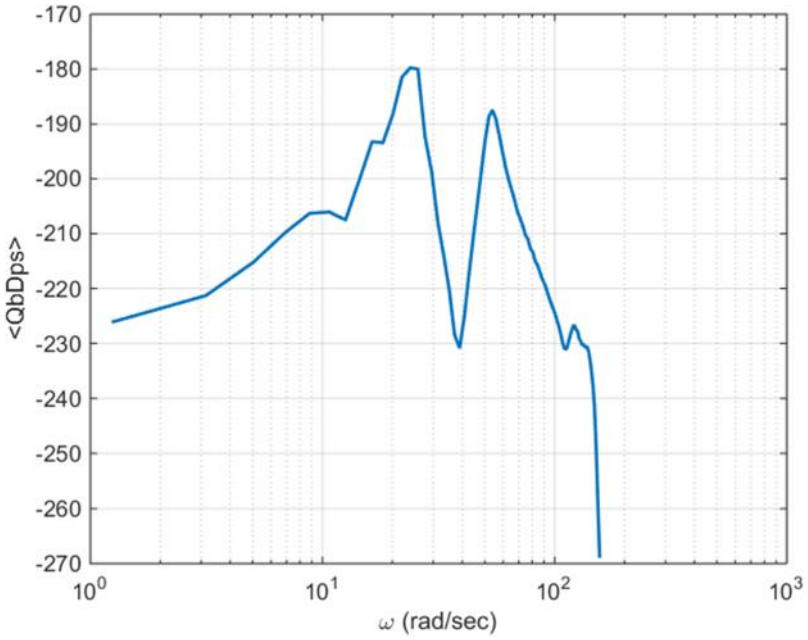

Figure 58: Power Spectral Density of Pitch Rate to Aileron Chirp Input.

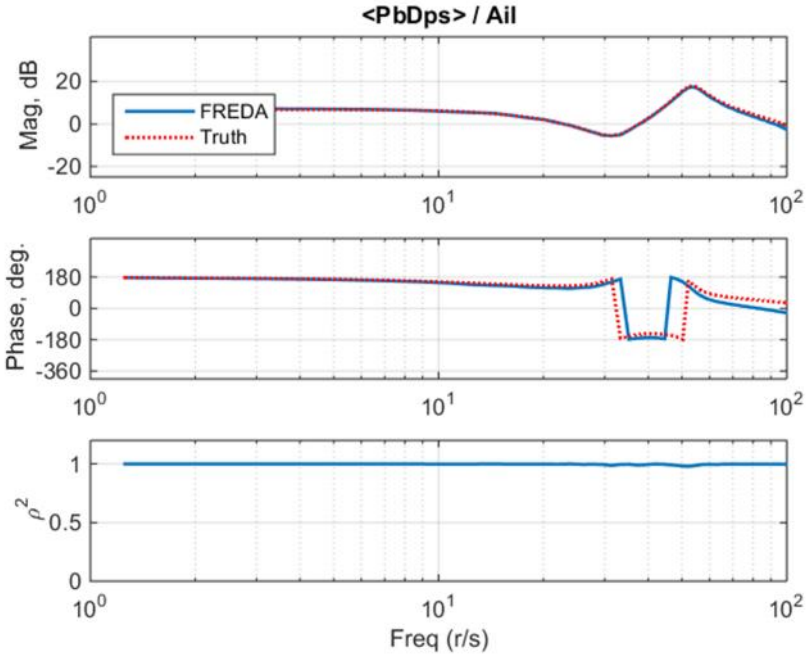

Figure 59: Frequency Response of Roll Rate to Aileron Chirp Input.

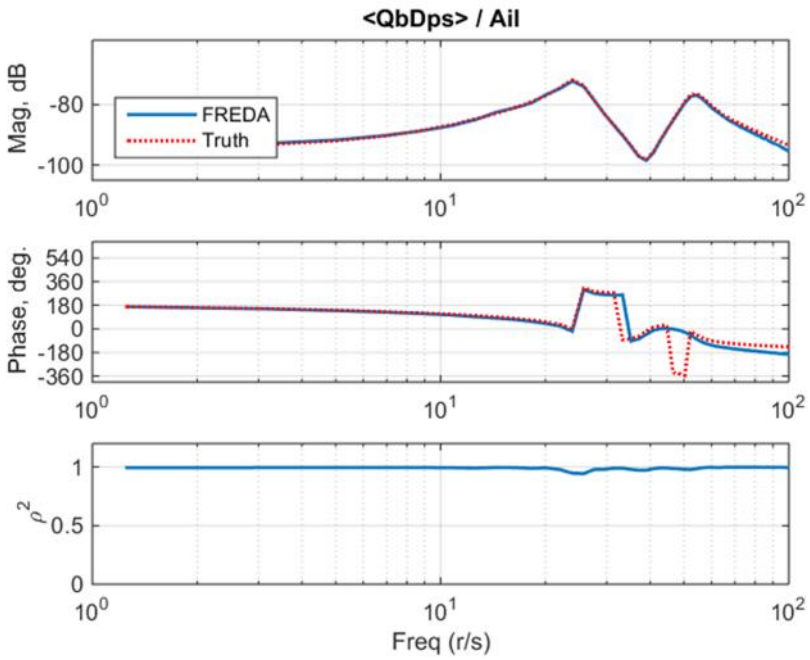

Figure 60: Frequency Response of Pitch Rate to Aileron Chirp Input.

(c) Elevator and Aileron Chirp Signal at the same time

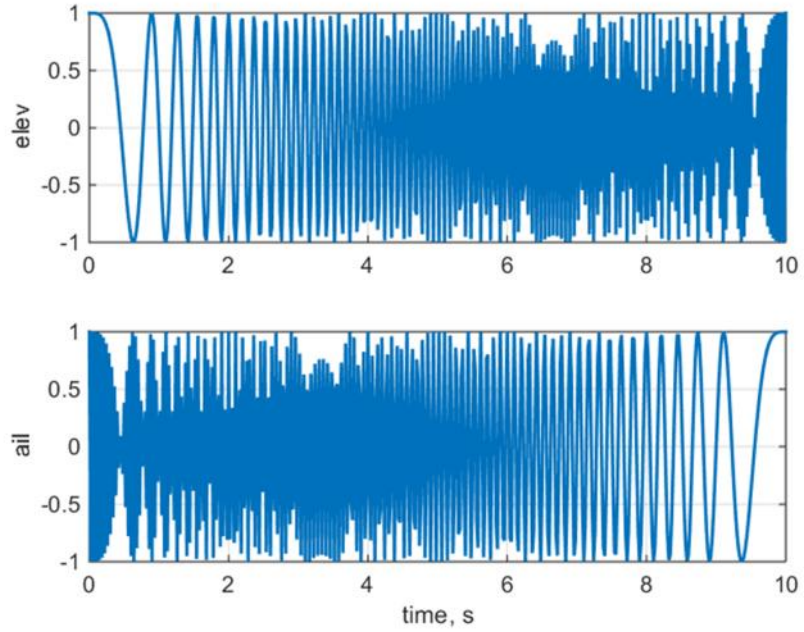

Figure 61: Control Input Time Histories.

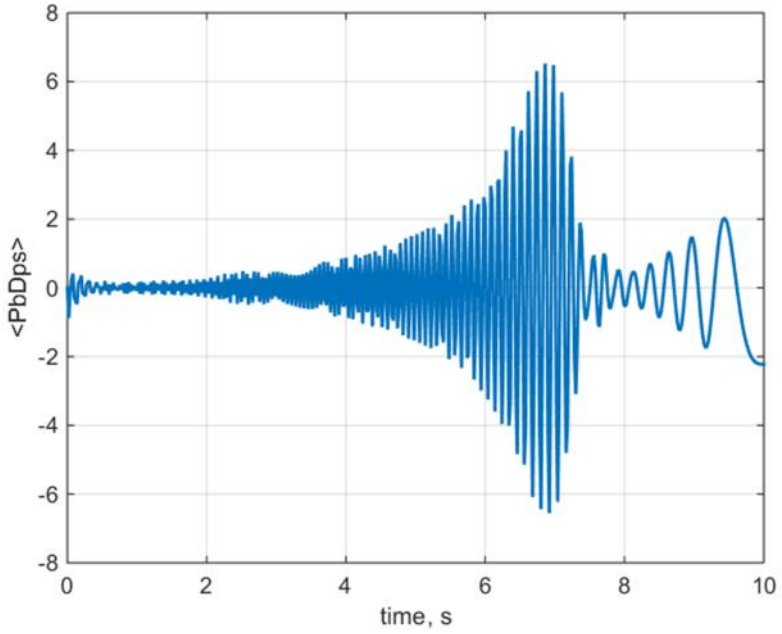

Figure 62: Roll Rate Response to Elevator and Aileron Chirp Inputs.

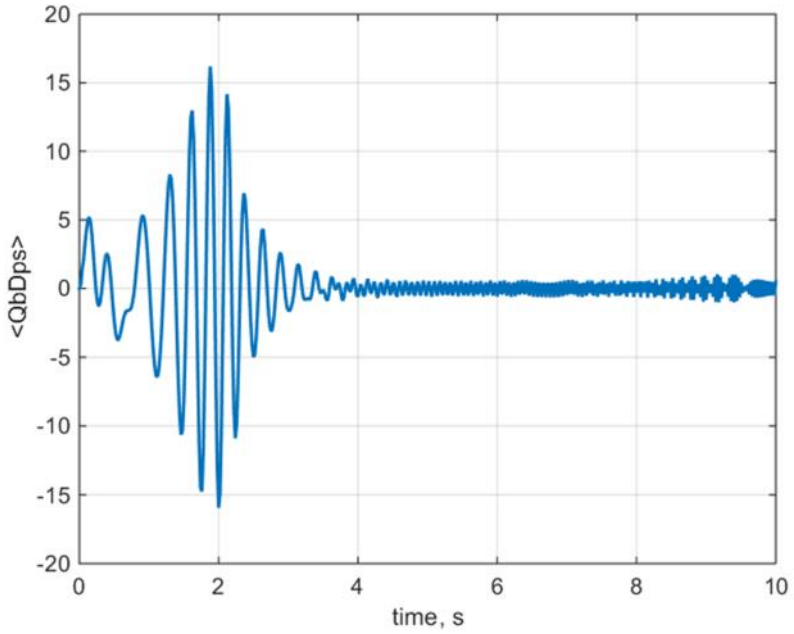

Figure 63: Pitch Rate Response to Elevator and Aileron Chirp Inputs.

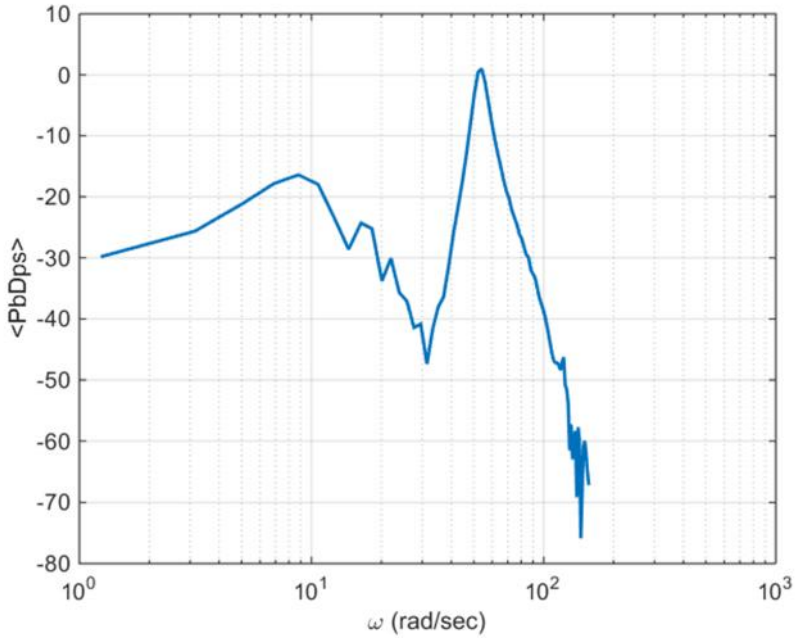

Figure 64: Power Spectral Density of Roll Rate to Elevator and Aileron Chirp Inputs.

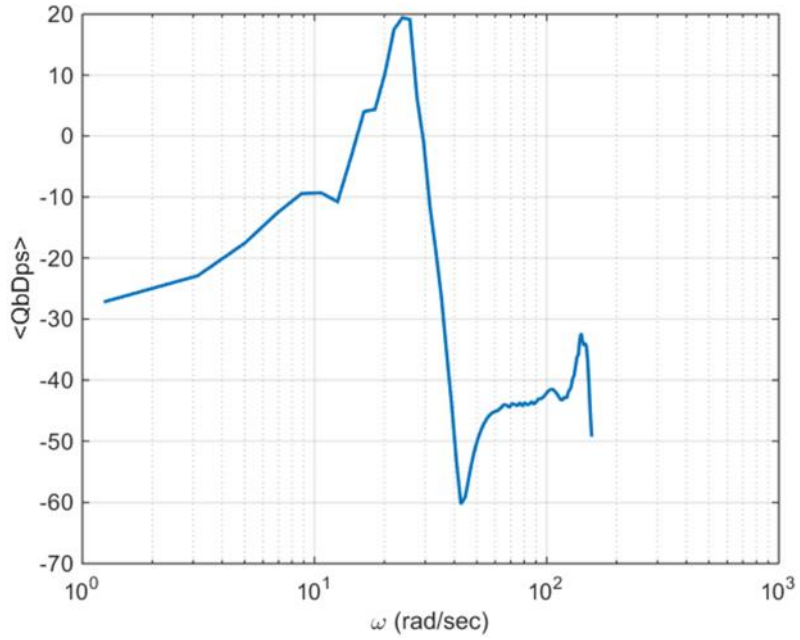

Figure 65: Power Spectral Density of Pitch Rate to Elevator and Aileron Chirp Inputs.

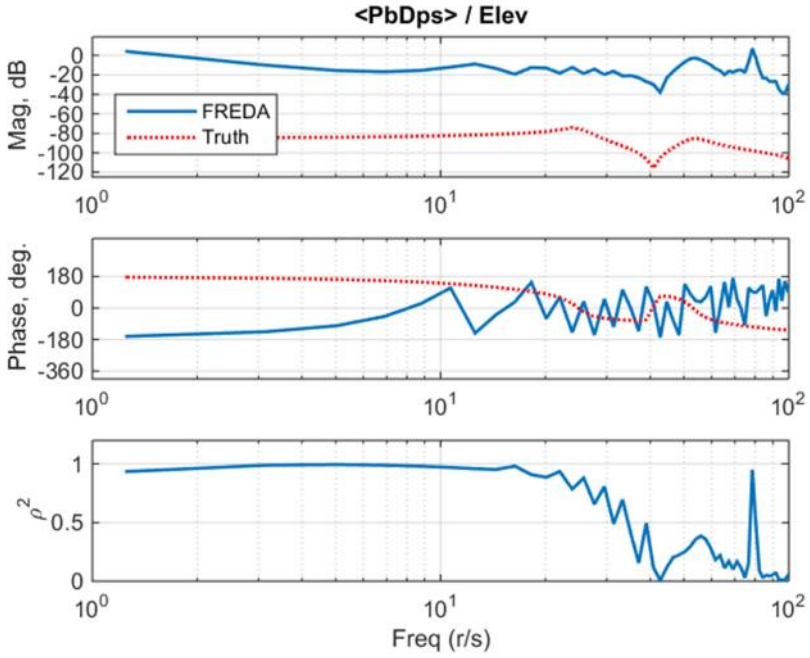

Figure 66: Frequency Response of Roll Rate to Elevator and Aileron Chirp Inputs.

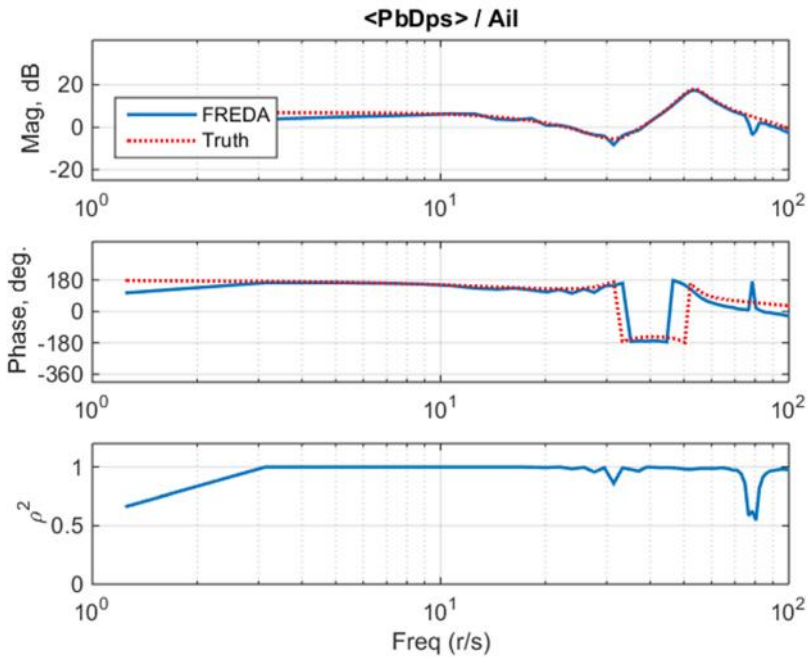

Figure 67: Frequency Response of Roll Rate to Elevator and Aileron Chirp Inputs.

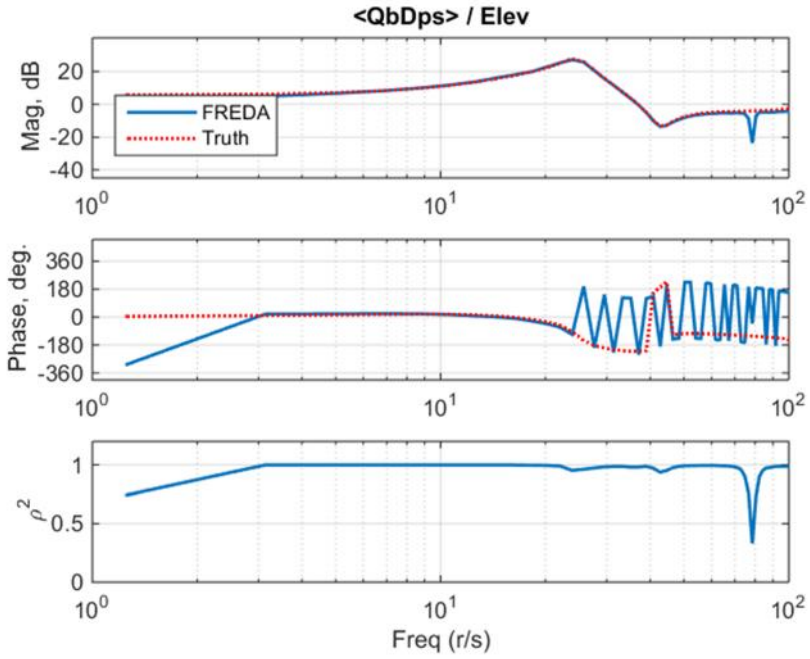

Figure 68: Frequency Response of Pitch Rate to Elevator and Aileron Chirp Inputs.

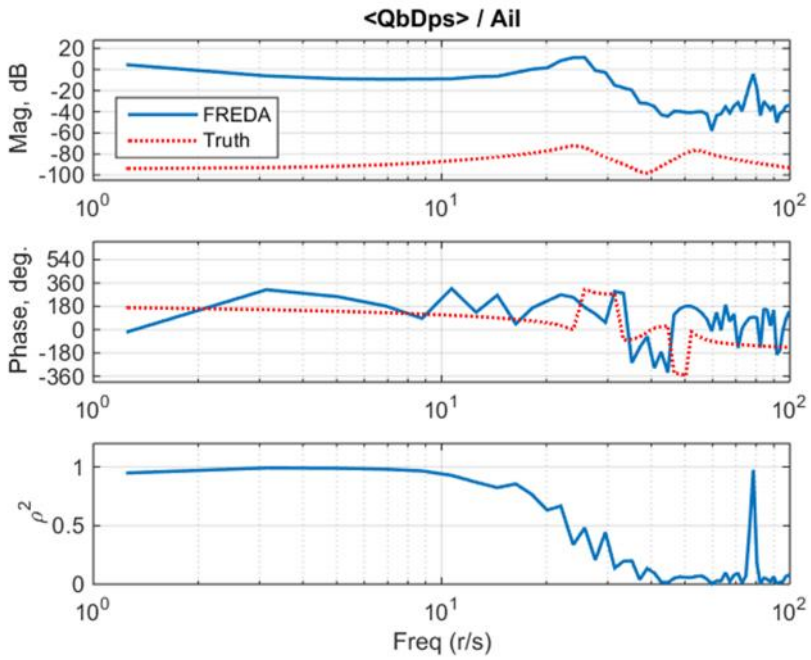

Figure 69: Frequency Response of Pitch Rate to Elevator and Aileron Chirp Inputs.

(2) Using Orthogonal Multi-Axis Sine Inputs for 3 seconds

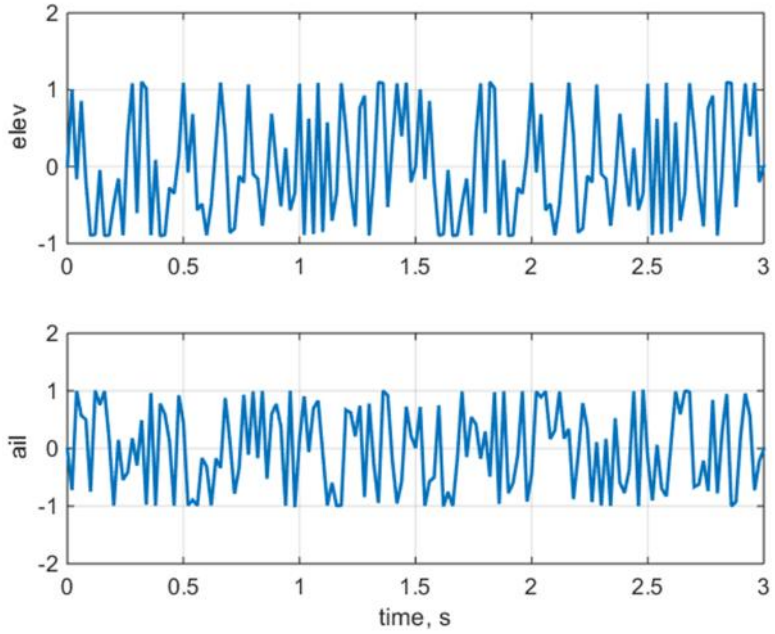

Figure 70: Control Input Time Histories.

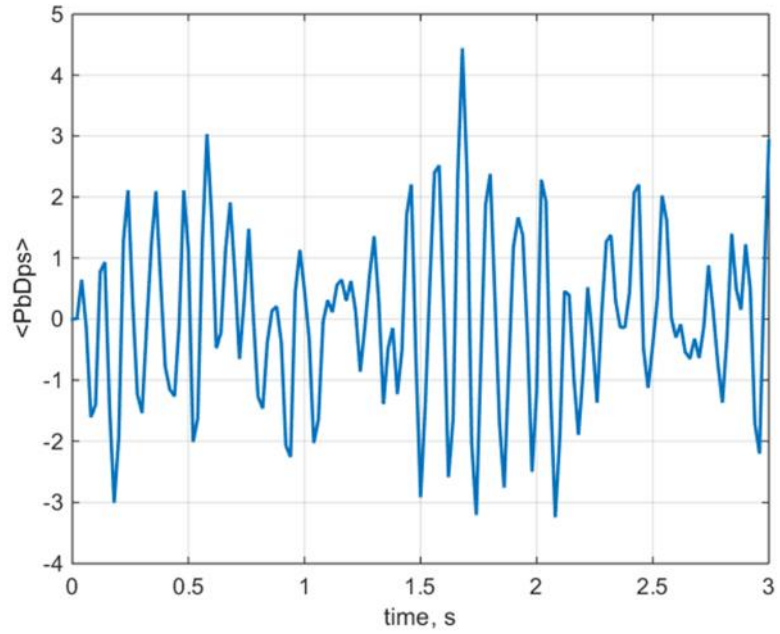

Figure 71: Roll Rate Response to Orthogonal Multi-Sine Sweep Elevator and Aileron Inputs.

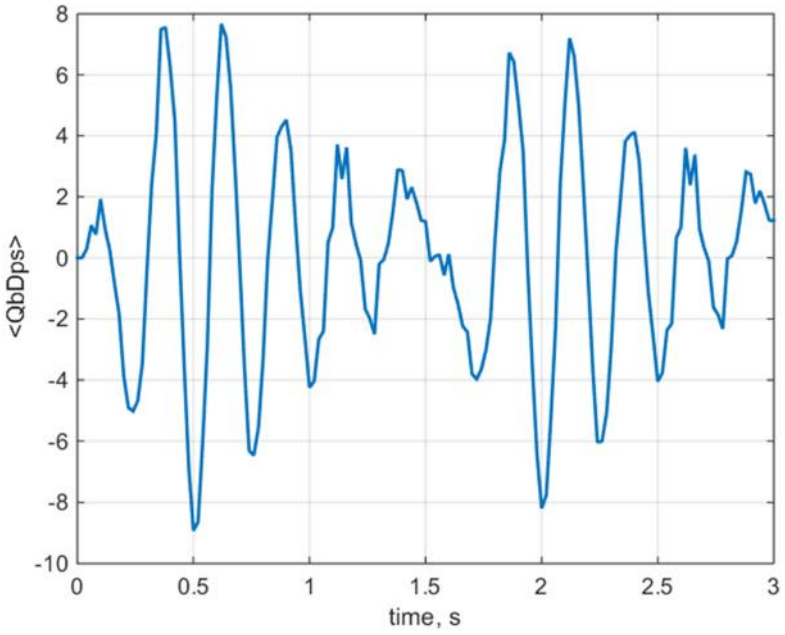

Figure 72: Pitch Rate Response to Orthogonal Multi-Sine Sweep Elevator and Aileron Inputs.

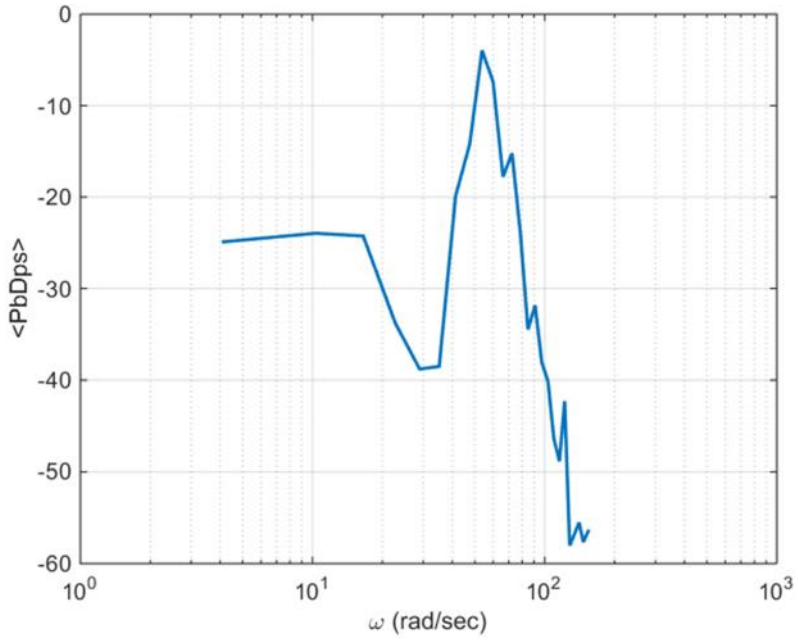

Figure 73: Power Spectral Density of Roll Rate to Orthogonal Multi-Sine Sweep Elevator and Aileron Inputs.

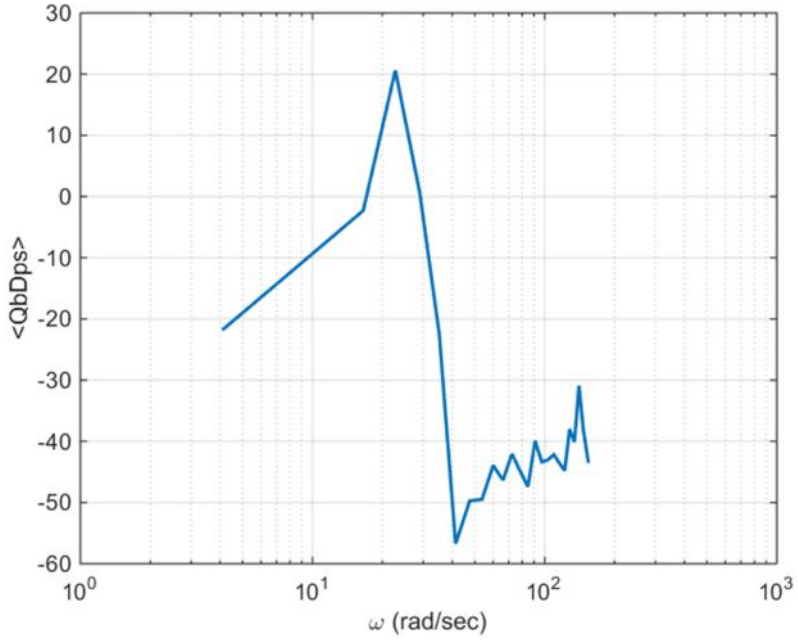

Figure 74: Power Spectral Density of Pitch Rate to Orthogonal Multi-Sine Sweep Elevator and Aileron Inputs.

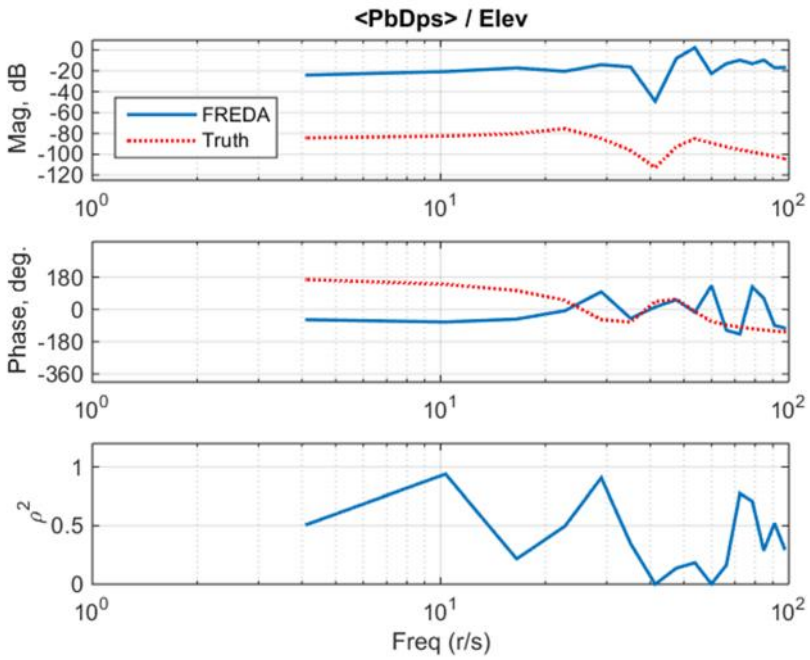

Figure 75: Frequency Response of Roll Rate to Orthogonal Multi-Sine Sweep Elevator and Aileron Inputs.

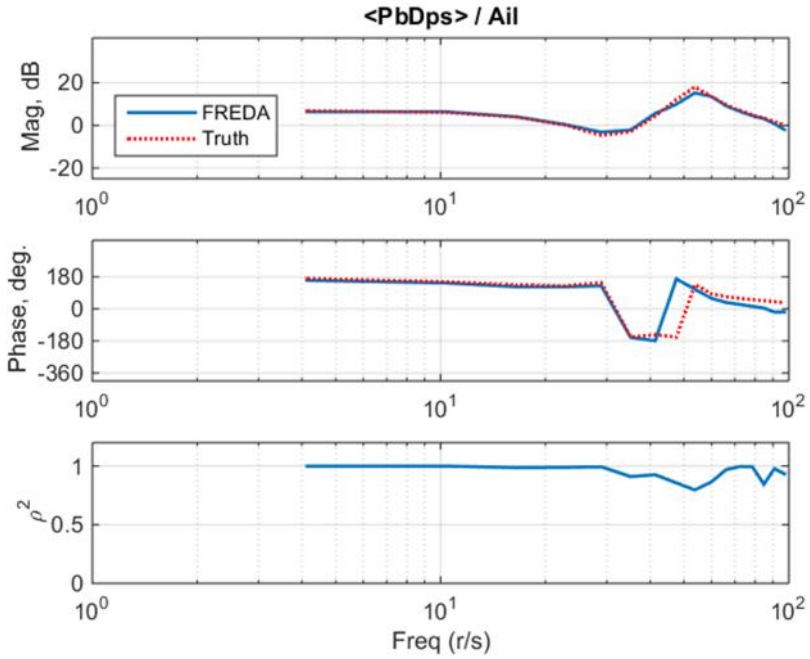

Figure 76: Frequency Response of Roll Rate to Orthogonal Multi-Sine Sweep Elevator and Aileron Inputs.

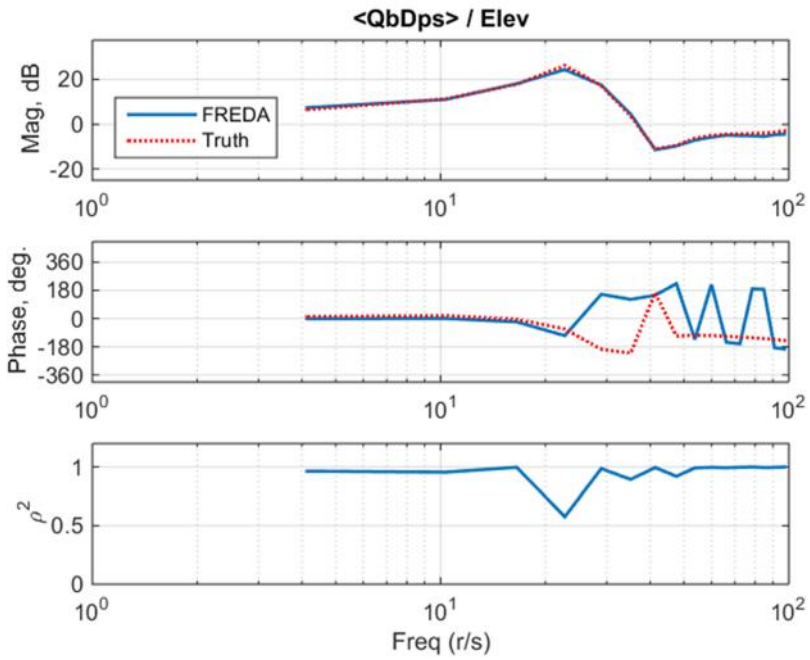

Figure 77: Frequency Response of Pitch Rate to Orthogonal Multi-Sine Sweep Elevator and Aileron Inputs.

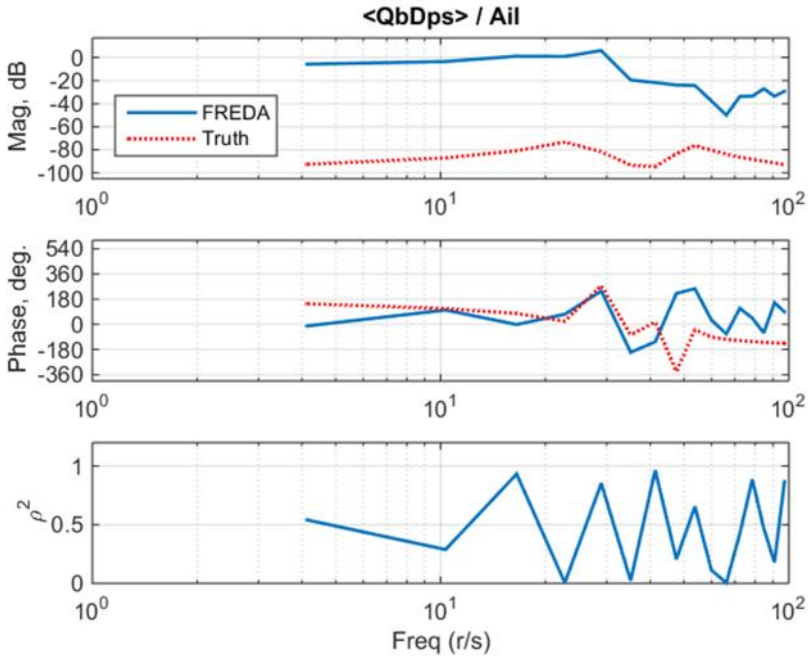

Figure 78: Frequency Response of Pitch Rate to Orthogonal Multi-Sine Sweep Elevator and Aileron Inputs.

(3) Elevator and Aileron 3-2-1-1 Inputs
(a) Elevator 3-2-1-1 Inputs

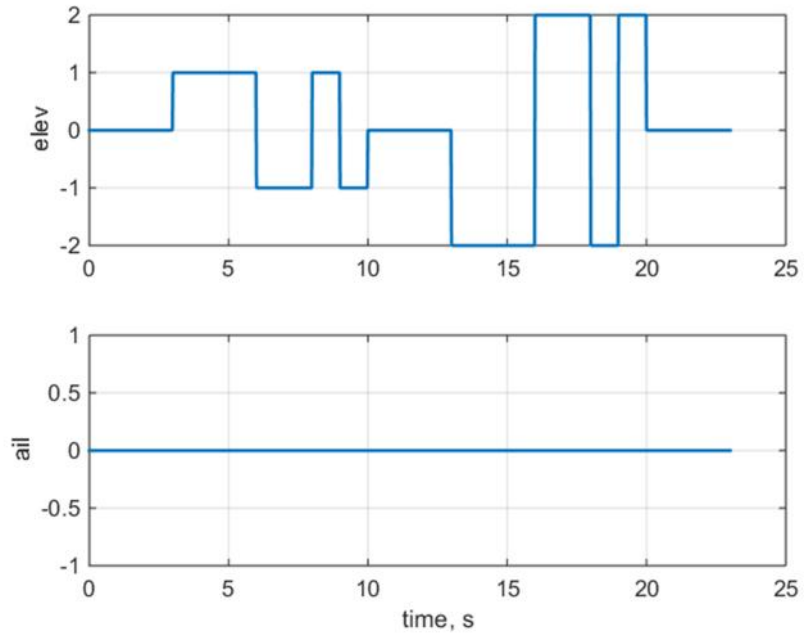

Figure 79: Control Input Time Histories.

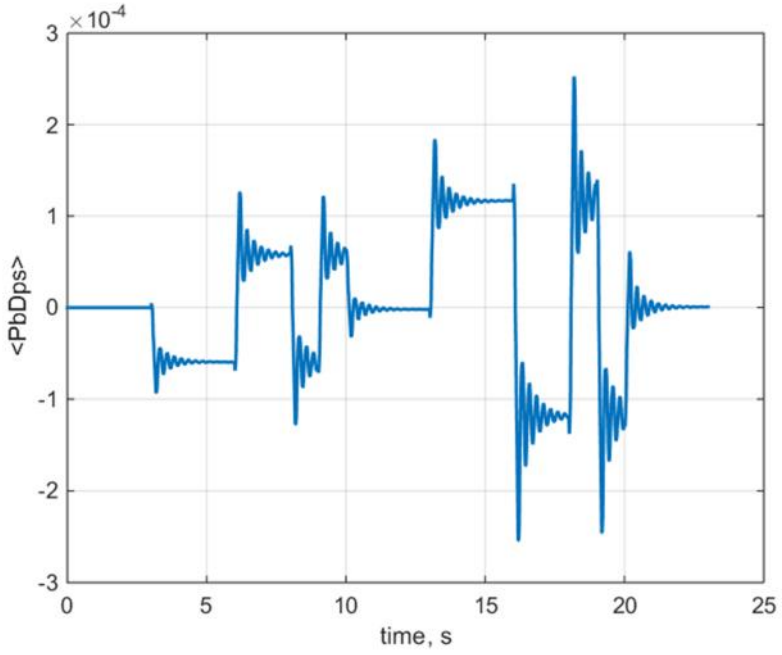

Figure 80: Roll Rate Response to Elevator 3-2-1-1 Input.

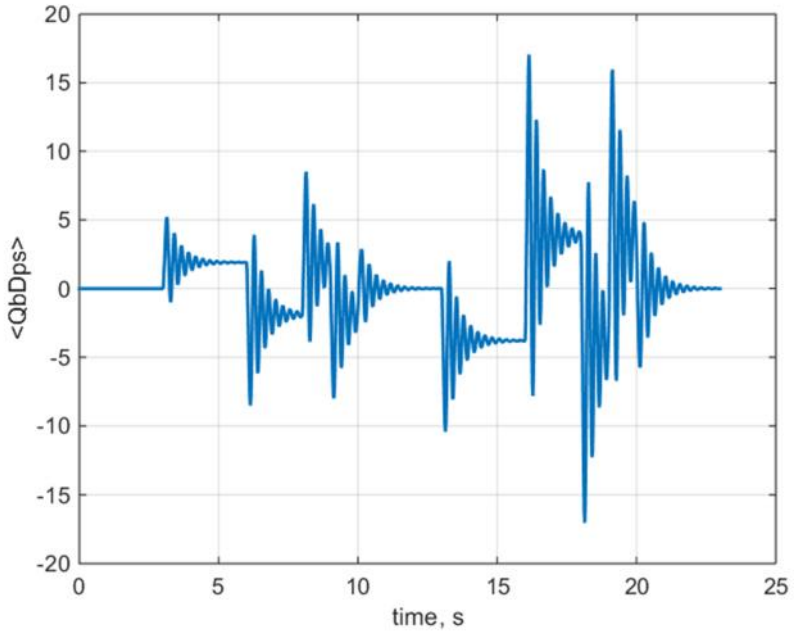

Figure 81: Pitch Rate Response to Elevator 3-2-1-1 Input.

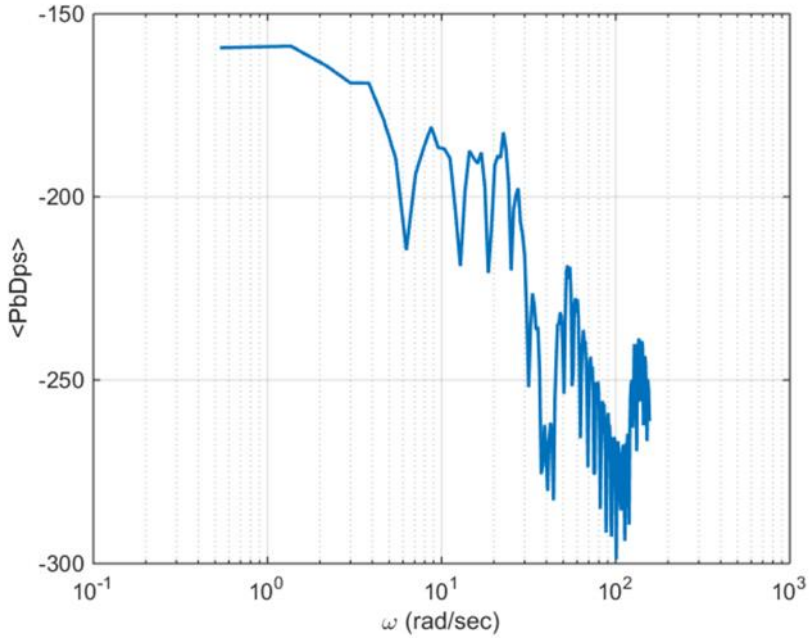

Figure 82: Power Spectral Density of Roll Rate to Elevator 3-2-1-1 Input.

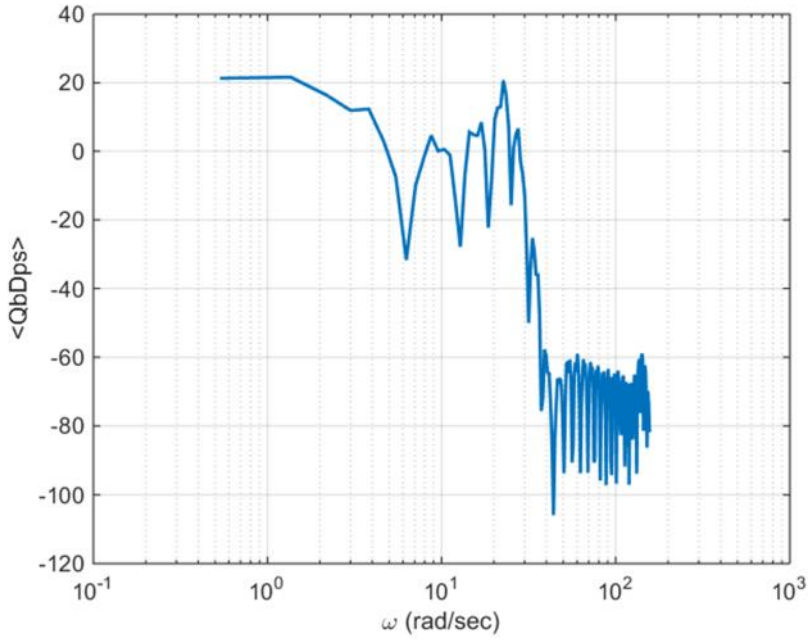

Figure 83: Power Spectral Density of Pitch Rate to Elevator 3-2-1-1 Input.

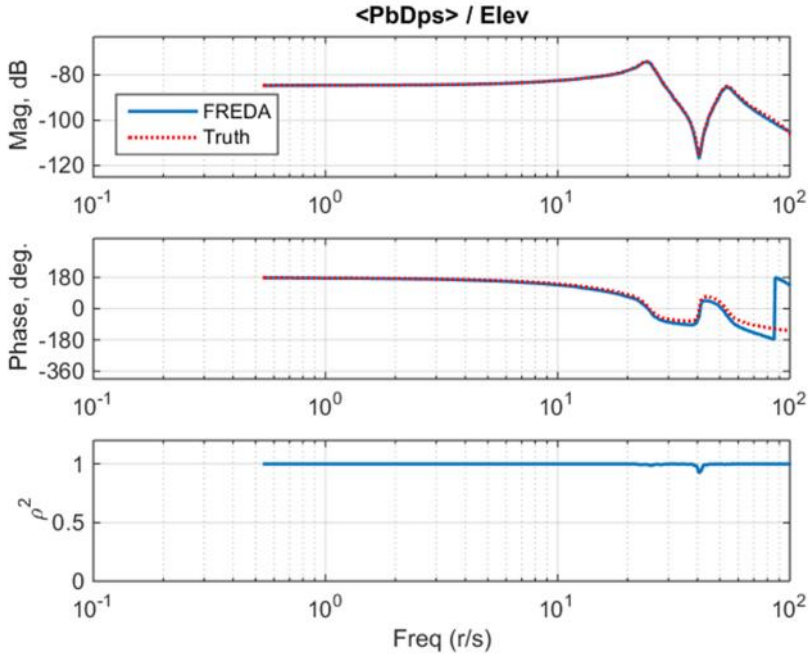

Figure 84: Frequency Response of Roll Rate to Elevator 3-2-1-1 Input.

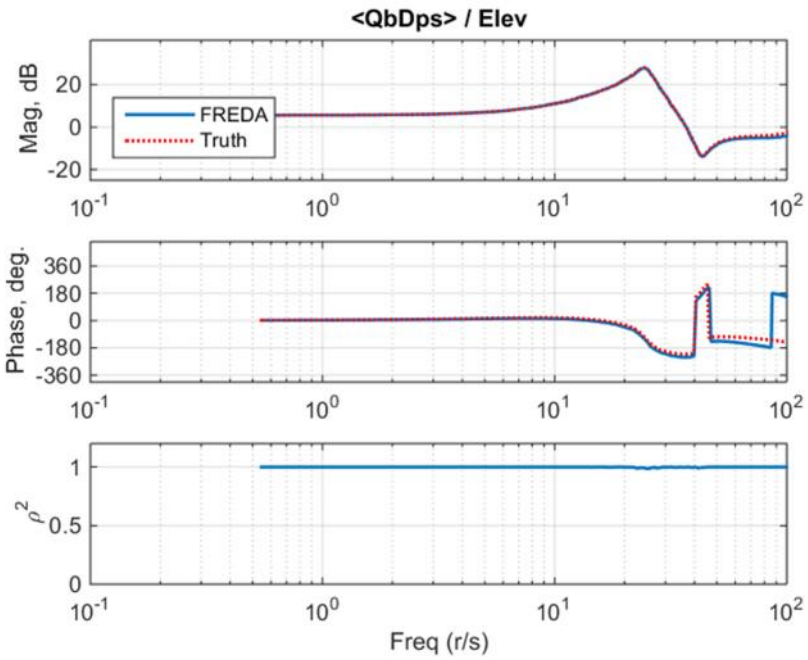

Figure 85: Frequency Response of Pitch Rate to Elevator 3-2-1-1 Input.

(b) Aileron 3-2-1-1 Input Only

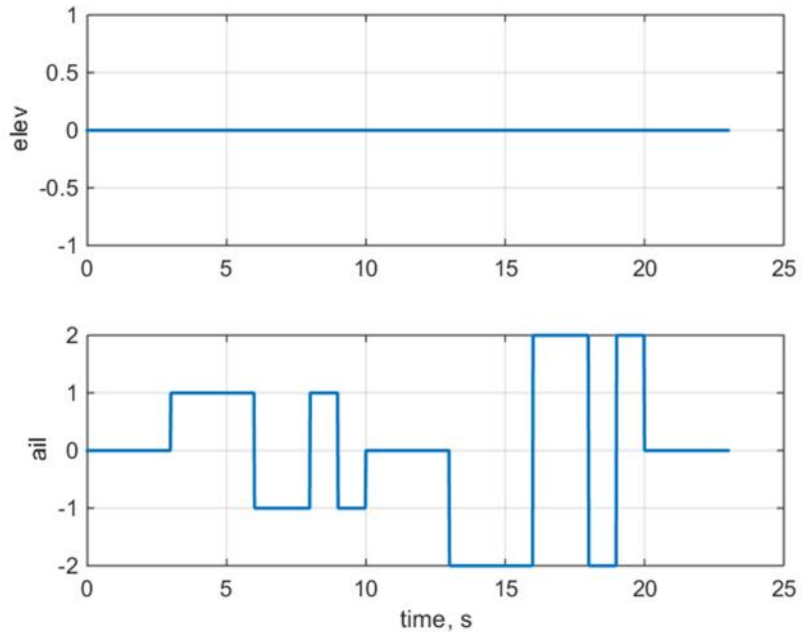

Figure 86: Control Input Time Histories.

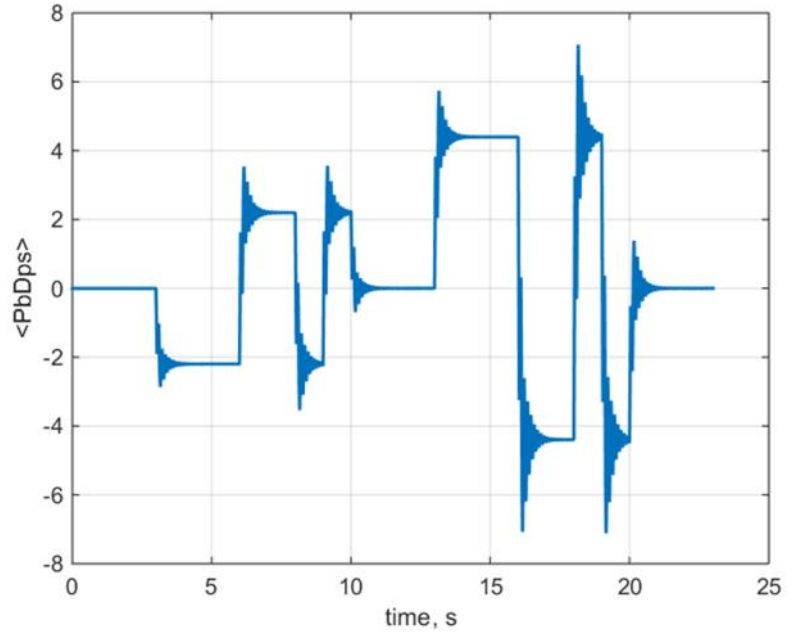

Figure 87: Roll Rate Response to Aileron 3-2-1-1 Input.

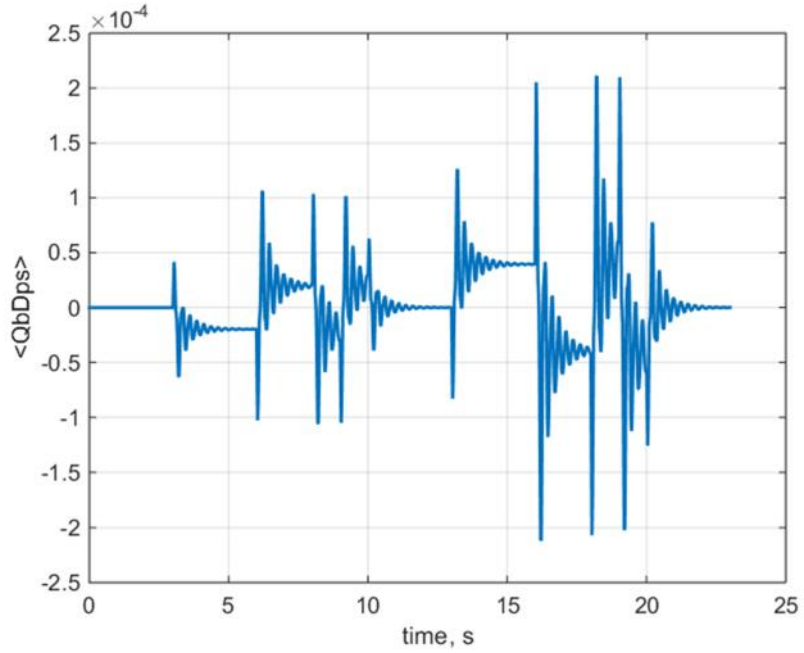

Figure 88: Pitch Rate Response to Aileron 3-2-1-1 Input.

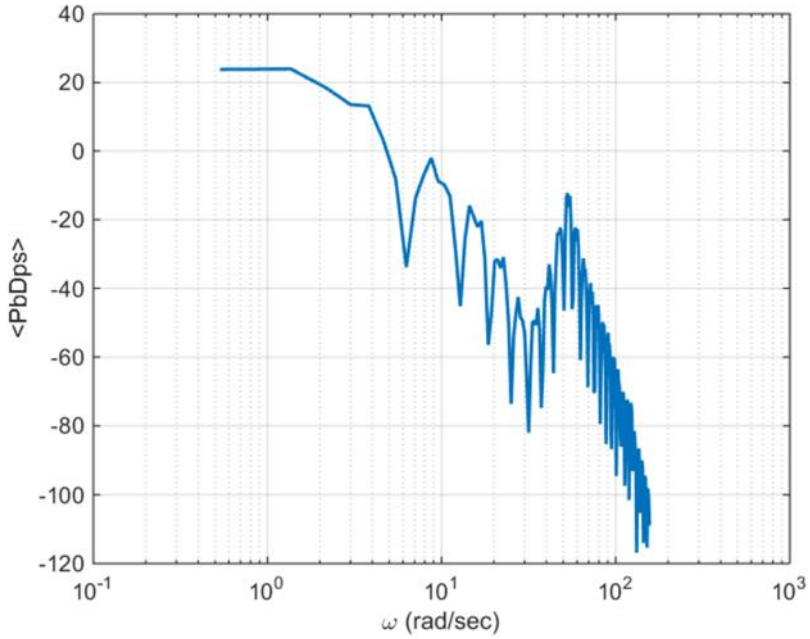

Figure 89: Power Spectral Density of Roll Rate to Aileron 3-2-1-1 Input.

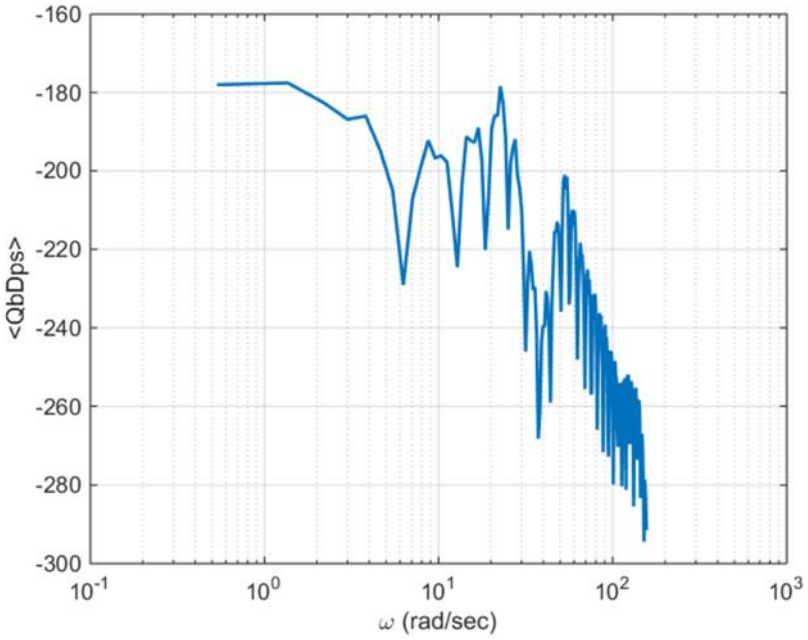

Figure 90: Power Spectral Density of Pitch Rate to Aileron 3-2-1-1 Input.

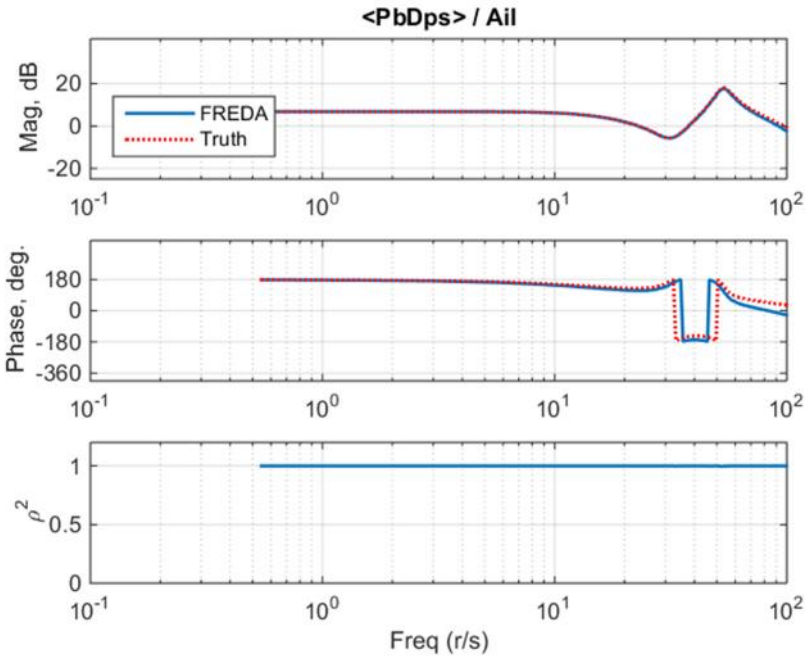

Figure 91: Frequency Response of Roll Rate to Aileron 3-2-1-1 Input.

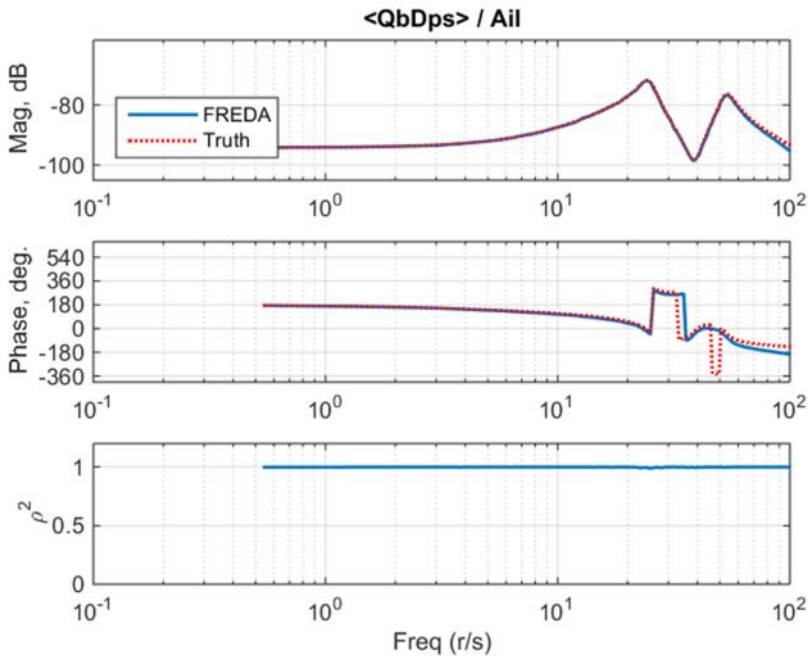

Figure 92: Frequency Response of Pitch Rate to Aileron 3-2-1-1 Input.